

Review

Critical Review of Wireless Charging Technologies for Electric Vehicles

Zhiwei Xue¹, Wei Liu^{2,3}, Chang Liu^{2,3} and K. T. Chau^{2,3,*} 

¹ Department of Electrical and Electronic Engineering, The University of Hong Kong, Hong Kong, China; zwxue@eee.hku.hk

² Research Centre for Electric Vehicles, The Hong Kong Polytechnic University, Hong Kong, China; wei.liu@polyu.edu.hk (W.L.); coeng.liu@connect.polyu.hk (C.L.)

³ Department of Electrical and Electronic Engineering, The Hong Kong Polytechnic University, Hong Kong, China

* Correspondence: k.t.chau@polyu.edu.hk

Abstract: As the world transitions towards sustainable transportation, the advancement of electric vehicles (EVs) has become imperative. Wireless power transfer (WPT) technology presents a promising solution to enhance the convenience and efficiency of EV charging while alleviating the challenges associated with traditional wired systems. This paper conducts an in-depth exploration of WPT technologies for EVs, focusing on their theoretical foundations, practical implementation, optimization strategies, development trends, and limitations. The theoretical principles of wireless charging are first elucidated, categorizing them into near-field methods, such as inductive and capacitive charging, and far-field methods, including microwave and laser-based charging. A comparative analysis reveals the advantages and limitations inherent to each technology. The implementation section examines various charging strategies, encompassing stationary, dynamic, and quasi-dynamic wireless charging, assessing their feasibility and effectiveness in practical applications. Furthermore, optimization techniques aimed at enhancing WPT system performance are examined in depth, with particular emphasis on coil structure optimizations, anti-misalignment solutions, compensation topology optimizations, modulation strategy optimizations, and parameter identifications. The discussion section outlines current development trends in wireless charging technologies for EVs, highlighting the limitations that hinder the widespread adoption of wireless charging technologies in the EV market. Finally, potential research directions and the implications of wireless charging technology on the development of EVs are summarized. This critical review aims to provide valuable insights for researchers and practitioners dedicated to advancing the field of wireless charging for EVs.

Keywords: wireless charging; electrical vehicles; inductive power transfer; capacitive power transfer; stationary-charging; dynamic-charging



Academic Editor: Peter Van den Bossche

Received: 31 December 2024

Revised: 17 January 2025

Accepted: 20 January 2025

Published: 22 January 2025

Citation: Xue, Z.; Liu, W.; Liu, C.; Chau, K.T. Critical Review of Wireless Charging Technologies for Electric Vehicles. *World Electr. Veh. J.* **2025**, *16*, 65. <https://doi.org/10.3390/wevj16020065>

Copyright: © 2025 by the authors. Published by MDPI on behalf of the World Electric Vehicle Association. Licensee MDPI, Basel, Switzerland. This article is an open access article distributed under the terms and conditions of the Creative Commons Attribution (CC BY) license (<https://creativecommons.org/licenses/by/4.0/>).

1. Introduction

The rapid proliferation of electric vehicles (EVs) signifies a profound transformation within the automotive industry, driven by an urgent need for sustainable transportation solutions and a reduction in reliance on fossil fuels. According to the “Global EV Outlook 2024” published by the International Energy Agency (IEA) [1], EV sales are poised for continued growth. In 2023, global EV sales reached approximately 14 million units and are expected to reach around 17 million by the end of 2024, accounting for more than

one-fifth of global car sales. EVs will become mainstream products in more countries. In the first quarter of 2024, EV sales increased by about 25% compared to the same period in 2023, mirroring the growth rate from 2022. With intense competition among automakers, declining prices for EV batteries and vehicles, and ongoing policy support, EV market penetration could reach 45% in China, 25% in Europe, and over 11% in the United States by 2024.

As global demand for EVs continues to rise, the quest for efficient, convenient, and user-friendly charging solutions becomes increasingly vital [2]. Wireless power transfer (WPT) technology emerges as one of the most promising innovations in this domain [3], [4]. It transmits electrical energy without the need for physical connections, offering an alternative to traditional plug-in charging methods.

WPT technology transmits energy through the air, eliminating the hassle of wiring [5]. Its notable feature is the ability to provide users with a seamless charging experience, addressing challenges faced by traditional charging infrastructure, such as the inconvenience of physically accessing charging stations and handling cables [6]. This approach not only streamlines the charging process but also enables the possibility of charging electric vehicles while in motion. Dynamic wireless charging technology allows vehicles to charge while in motion via embedded road charging devices, significantly alleviating range anxiety—a primary barrier to widespread EV adoption [7]. By integrating WPT technology into urban infrastructure, cities can create a more EV-friendly ecosystem, thereby promoting the adoption and use of EVs.

On a technical level, WPT technology is categorized into near-field and far-field WPTs [8], where the inductive power transfer system of near-field WPT shows great potential for EV charging [9]. Specifically, static charging solutions in parking lots allow EVs to charge automatically while parked, providing greater convenience for users. Additionally, dynamic wireless charging on urban roads enables EVs to charge while in motion, effectively extending their driving range and reducing downtime. To enhance the charging efficiency, researchers are exploring ways to optimize coil design, improve power transfer efficiency, and reduce power loss [10]. Additionally, addressing vehicle and charging device misalignment is a key focus to ensure stable and reliable charging. Despite its advantages, WPT technology faces challenges in safely transmitting high-power energy without interfering with other electronics and achieving standardization across various vehicle models and manufacturers. These issues necessitate further research and international collaboration.

This review aims to conduct an in-depth evaluation of various wireless charging technologies applicable to EVs, categorizing them into near-field and far-field methods. Within these categories, inductive and capacitive charging technologies, as well as microwave- and laser-based systems, will be explored for a comprehensive understanding of their theoretical principles and practical applications. Furthermore, different EV wireless charging modes, including stationary, dynamic, and quasi-dynamic systems, will be analyzed in detail to highlight their potential to enhance the EV charging ecosystem. Additionally, optimization strategies aimed at improving the performance of wireless charging systems will be conducted, focusing on advancements in coil structure design, mechanisms to counteract misalignment, advanced compensation networks, modulation methods to enhance system efficiency, and the identification of key parameters. Finally, a broader discussion of current trends and limitations in EV wireless charging technology will be given. By synthesizing existing research and emphasizing future directions, this paper aims to provide valuable insights for the ongoing development of wireless charging systems, ultimately supporting the transition to a more sustainable and convenient EV landscape.

2. Theoretical Principle of Wireless Charging Technologies

WPT is a technology that utilizes a transmitter to convert electrical energy into another form of relay energy (e.g., electromagnetic field energy, lasers, and microwaves) and then transmits the relay energy over certain distances and then converts it back into electrical energy through a receiver, thus achieving wireless power transmission. Currently, the mainstream WPT technologies can be classified into three main categories based on the type of relay energy as follows: magnetic coupling, electric field coupling, and electromagnetic radiation [11]. In addition, WPT can be categorized based on the distance from the transmitter and receiver, typically using a wavelength as the dividing criterion. This classification distinguishes between the near-field WPT and far-field WPT [12], as shown in Figure 1.

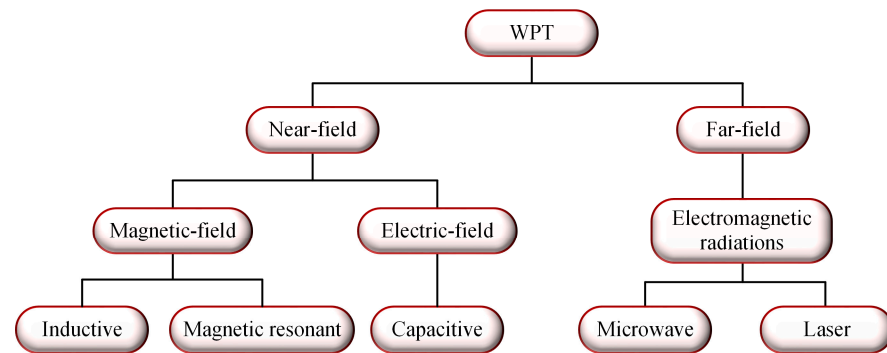


Figure 1. Classification of WPT based on different criteria.

2.1. Near-Field Wireless Charging

Near-field WPT technologies utilize the near-field effect of electromagnetic fields, which can be divided into the following two main methods: magnetic field coupling and electric field coupling [13]. Magnetic field-coupled WPT can be further subdivided into inductive power transfer (IPT) [14] and magnetic resonance WPT (MR-WPT) [15]. In the near-field region, energy is concentrated within the localized vicinity of the transmitter. If the receiver is not positioned correctly or within an effective range, efficient coupling between the receiver and transmitter cannot be achieved, hindering effective power transfer. The effective range of near-field WPT depends on the physical dimensions of the transmitter and receiver and the degree of coupling. Moreover, electric field coupling realizes power transfer through high-frequency electric fields, while magnetic field coupling utilizes high-frequency alternating magnetic fields [16]. Notably, electric field coupling is subject to stringent distance limitations, whereas magnetic field coupling, especially MR-WPT, demonstrates the capability to transmit energy over greater distances, showcasing enhanced flexibility and practicality in real-world applications [17].

2.1.1. Inductive Wireless Charging Technology

Inductive power transfer (IPT) is a wireless charging technology based on the principle of electromagnetic induction [18]. Its fundamental operation involves the following two primary components: the transmitter coil and the receiver coil. The transmitter coil generates a varying magnetic field through alternating current, which, according to Faraday's law of electromagnetic induction, induces an electromotive force in the receiver coil, thereby generating current and enabling the wireless transfer of energy [19]. Figure 2 shows the schematic diagram of the IPT system, where the transmitter-side high-frequency alternating current is generated by the inverter, and then the high-frequency alternating current produced by the receiver coil is converted into direct current by a rectifier to charge a load, such as a battery [20].

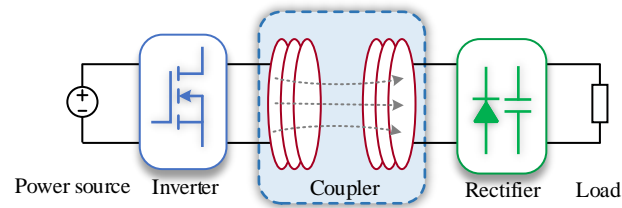


Figure 2. Principle of inductive power transfer (IPT).

The advantages of IPT lie in its efficient and reliable energy transmission capabilities, particularly suited for short-distance charging. The efficiency of energy transfer depends on the degree of alignment and distance between the coils, with optimal performance typically achieved when their relative positions are favorable [21]. In addition, the design of IPT systems is relatively straightforward, effectively preventing contact wear and enhancing the reliability of the equipment. However, as the distance increases, the transmission efficiency may decline significantly, thereby limiting its applications [22].

2.1.2. Magnetic Resonance Wireless Charging Technology

Magnetic resonance wireless power transfer (MR-WPT) is an emerging WPT technology that leverages the principle of electromagnetic resonance to achieve efficient power transfer over longer distances and at higher power levels [23]. The core of MR-WPT lies in the resonant design of the transmitter and receiver coils. As shown in Figure 3, the coupling mechanism resembles a loosely coupled transformer, with the distance between the coils being greater than in traditional IPT systems, typically resulting in a coupling coefficient below 0.3 [24]. When the transmitter coil generates a varying magnetic field through alternating current, the receiver coil can harness energy at the resonant frequency, thereby maximizing energy transfer efficiency. MR-WPT can transmit over distances of up to several meters, and its capability to penetrate walls and non-metallic obstacles enhances its flexibility in complex environments [25]. Furthermore, the efficient power transfer capabilities make MR-WPT suitable for applications in EVs, consumer electronics, and industrial settings, allowing simultaneous charging of multiple devices [26].

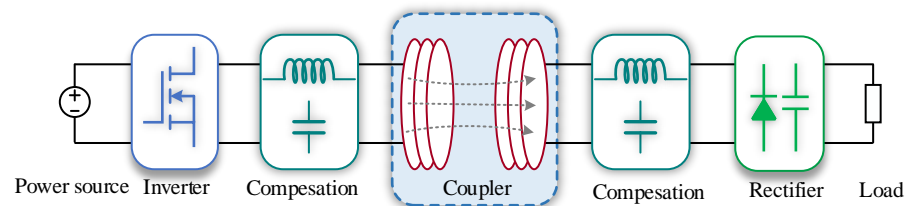


Figure 3. Principle of magnetic resonance wireless power transfer (MR-WPT).

The most advanced MR-WPT systems have achieved efficiencies exceeding 95%, rivaling traditional wired power transmission [27]. Additionally, power levels have reached hundreds of kilowatts, with megawatt capabilities attainable through the parallel use of multiple modules or the deployment of multi-phase systems [28]. Despite its significant advantages, the design and implementation of MR-WPT remain relatively complex, necessitating precise control of the resonant frequency and the relative positioning of the coils. As technology advances, MR-WPT is expected to play a pivotal role in future wireless charging solutions for electric vehicles.

2.1.3. Capacitive Wireless Charging Technology

The electric field-coupled WPT system is known as the capacitive power transfer (CPT) system [29]. A typical structure of a CPT system is illustrated in Figure 4, which

comprises a power supply, high-frequency inverter, resonant network at the transmitter end, coupling mechanism, resonant network at the receiver end, rectifier filter, and load [30]. CPT technology facilitates power transfer through electric field coupling by incorporating metallic plates on both the transmitter side and receiver side to form 2 capacitors. Under the excitation of high-frequency alternating voltage, displacement current is generated between the metallic plates. With the aid of the compensation network at the receiver side, electrical energy is converted into the desired output voltage and current, which is then rectified and filtered into direct current for the load, thereby enabling wireless energy transmission [31]. The use of aluminum plates as coupling mechanisms offers a cost-effective solution with strong resistance to misalignment [32]. However, electric field coupling also presents challenges such as limited transmission distances and potential hazards from leakage fields.

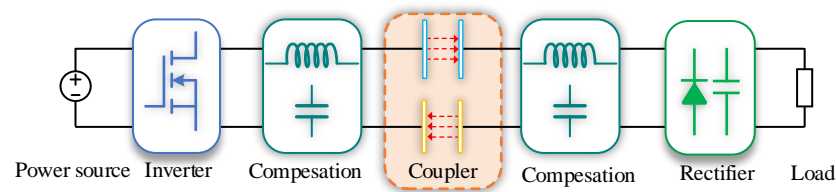


Figure 4. Principle of capacitive power transfer (CPT).

In addition, parallel plate capacitors typically possess a relatively small coupling capacitance, which negatively impacts the power transmission capability of CPT [33]. To address this issue, the CPT system described in [34] is capable of transmitting 2.4 kW of power across a 150 mm air gap. Additionally, Sinha et al. achieved a power transfer of 19.6 kW/m² at a 120 mm air gap and a resonant frequency of 6.78 MHz [35]. Overall, CPT technology can reach power transmission levels of several kilowatts. However, high-power CPT systems continue to face challenges.

To effectively supply power over larger air gaps, Zhang et al. successfully increased the operating frequency to 13.56 MHz, thereby boosting the power density to 29.5 kW/m² [36]. In contrast, MR-WPT technology can achieve a power density of up to 160 kW/m², with multi-phase magnetic couplers further enhancing this capability. One potential solution is to raise the operating frequency further; however, the ultra-high switching frequencies and high-power capabilities of power switches are constrained by existing semiconductor technology. Additionally, high-frequency operation inevitably subjects compensation components to excessive voltage and current stresses. The enhanced voltage tolerance of gallium nitride (GaN) switch technology is expected to drive the development of future high-power CPT systems [37,38].

It should be pointed out that CPT systems require two pairs of metal plates to form a complete electrical circuit for the power transfer from the transmitter to the receiver [39]. However, the use of two pairs of coupling plates often leads to the following issues:

1. The cross-coupling between multiple coupling plates becomes more pronounced as the coupling distance increases, adversely affecting power transfer efficiency.
2. When a metal obstacle spans the coupling region of the two pairs of plates, the system struggles to transmit power through the metal barrier.
3. The parallel coupling mechanism occupies considerable space, while the design of stacked coupling mechanisms is complex.

In contrast, a single-capacitor CPT system requires only one pair of coupling plates to achieve wireless power transmission, effectively overcoming the aforementioned challenges [40–42]. Its simplified circuit is illustrated in Figure 5. In a single-capacitor CPT system, only one metal plate is employed as an electrode at both the transmitter and receiver sides, effectively addressing the issues associated with dual coupling plates. Lu et al. uti-

lized the stray capacitance between the vehicle chassis and the ground to provide a current return path for power transmission, which can replace the two plates in traditional four-plate CPT systems, realizing wireless charging for electric vehicles using single-capacitor CPT technology [41]. Therefore, the coupling mechanism of single-capacitor CPT systems is simpler and more flexible, facilitating power transmission across metallic barriers [43]. Moreover, by using fewer components, manufacturing and deployment costs are reduced, and the simplified design makes the installation process more intuitive, lowering labor costs. Importantly, single-capacitor CPT can offer flexible charging solutions in space-constrained or complex environments. However, the transmission mechanism of single-capacitor CPT systems remains to be fully elucidated, necessitating a comprehensive analysis of its energy transfer mechanisms.

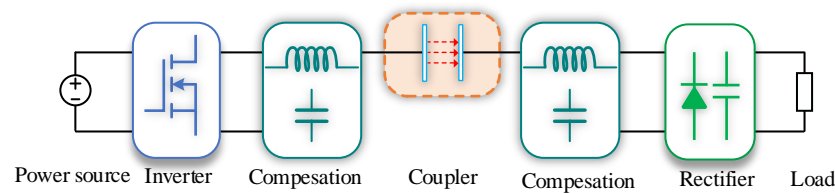


Figure 5. Principle of single-capacitor CPT.

2.2. Far-Field Wireless Charging

Electromagnetic radiation-based wireless power transfer technology has garnered widespread research interest due to its exceptional long-distance transmission capabilities [44]. This technology harnesses the far-field characteristics of electromagnetic waves, allowing power transfer distances to significantly exceed the dimensions of the devices themselves. Since energy radiates outward, precise energy transfer typically requires the use of directional devices to ensure accurate delivery. There are primarily two forms, namely, microwave power transfer (MWPT) and laser power transfer (LPT).

2.2.1. Microwave Wireless Charging Technology

Microwave wireless power transfer (MWPT) technology uses microwaves within electromagnetic waves to transmit power over long distances, as shown in Figure 6. A microwave power source converts direct current into microwaves, which are transmitted via an antenna into free space. The receiving antenna then captures these microwaves and converts them back into direct current through a rectifying circuit to charge batteries or power loads [45]. Power losses mainly occur due to environmental factors like obstructions and atmospheric dust. MWPT is notable for its long transmission distances and high-power capacity, making it suitable for medium- to long-range applications [46]. Research into 2.45 GHz microwave technology began as early as 1988, initially powering model airplanes. Subsequent explorations have included applications such as space-based solar power stations, microwave-powered aircraft, and interisland wireless energy transmission, highlighting the potential of microwave technology in various scenarios [47].

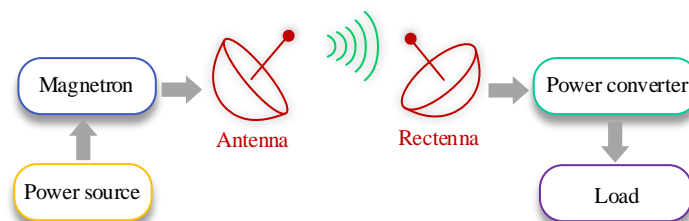


Figure 6. Principle of microwave power transfer (MWPT).

2.2.2. Laser Wireless Charging Technology

Laser power transfer (LPT) technology uses lasers for wireless energy transmission over medium to long distances [48]. The process involves powering a laser with electricity, which converts electrical energy into laser light. This laser is directed onto a photovoltaic array, where a photovoltaic converter transforms the laser light into electrical energy for charging storage devices, as shown in Figure 7. LPT systems offer advantages such as small transmission and reception apertures, high flexibility, elevated energy density, good directionality, and immunity to electromagnetic interference (EMI). However, overall efficiency can be impacted by tracking precision and atmospheric conditions [49]. Safety measures are also essential to prevent hazards and energy loss from misdirected laser beams [50].

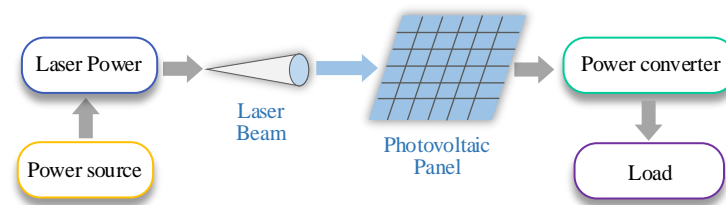


Figure 7. Principle of laser power transfer (LPT).

2.3. Comparative Analysis

The fundamental principles of IPT and MR-WPT are increasingly viewed as identical, differing only in the use of resonant networks. Both fall under the category of magnetic coupling wireless power transfer technology [51]; therefore, this discussion will refer to both collectively as IPT. In this technology, resonance at the transmitter side can enhance power transfer, while resonance at the receiver side can improve transmission efficiency [52]. Moreover, IPT also presents several challenges:

1. To mitigate the effects of proximity and skin effect, high-frequency Litz wire is typically used to wind the coils, necessitating magnetic core structures and aluminum plates to reduce magnetic field leakage and avoid external interference, which results in higher material costs.
2. The high-frequency magnetic fields generated can induce eddy currents in metals, leading to energy losses.
3. This technology lacks the ability to penetrate metal barriers.
4. The coupling coils have low redundancy in terms of positional offset; when the coil positions shift, significant power fluctuations can occur, interfering with the normal operation of power electronic converters and requiring specialized designs to counteract positional shifts.

CPT technology employs alternating electric fields as the medium for wireless energy transfer, utilizing 2 coupled capacitors formed from plate-like electrodes on both the transmitter and receiver sides as the energy transmission path. The advantages of CPT technology include a simple coupling mechanism, low cost, and insensitivity to surrounding metallic objects [53]. Nevertheless, CPT also has its limitations, such as high voltage stress and short transmission distances.

In comparison to near-field WPT technologies, electromagnetic radiation-based WPT demonstrates clear advantages in transmission power and efficiency over longer distances. However, until safety concerns regarding electromagnetic radiation are adequately addressed, the use of far-field WPT for charging EVs remains impractical [54]. Table 1 provides a detailed comparison of the above WPT technologies, including the advantages and disadvantages of each method.

Table 1. Comparison of different WPT technologies.

WPT Methods		Advantages	Disadvantages
Near-field WPT	Inductive	Simple structure High efficiency at short range Relatively safe	Short transmission distance Low efficiency at long range High alignment requirements
	Magnetic resonant	Relatively long transfer range Misalignment insensitive High efficiency and power level	Heat dissipation issues EMI issues Relatively high cost
	Capacitive	Medium power transmission Lightweight coupler Power transfer through metal	High resonant frequency Cumbersome coupler with 4 plates High voltage and current stress
Far-field WPT	Microwave	Long transfer distances High-power possibilities Highly efficient possibilities	High cost and difficult to implement No bidirectional transmission Biologically unsafe
	Laser	Long transfer range High-power possibilities Small transmitter and receiver	Biological unsafety Low efficiency Vulnerability to obstacles

Note: EMI: electromagnetic interference.

3. Implementation of Wireless Charging for EVs

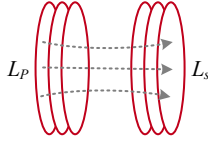
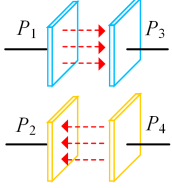
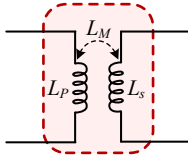
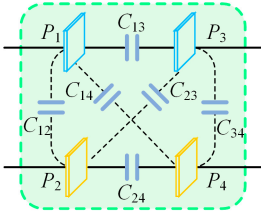
Wireless charging technology for electric vehicles (EVs) mainly includes the following three forms: stationary, dynamic, and quasi-dynamic [55]. Stationary wireless charging requires the EVs to be parked over a charging platform, where energy transfer is realized by coupling electric or magnetic fields between the transmitting and receiving units. This approach is straightforward and widely implemented [56]. Dynamic wireless charging allows EVs to charge in real-time while in motion, making it suitable for public transportation systems. It can significantly extend the vehicle's range; however, it comes with high implementation costs and demanding infrastructure requirements [57]. Quasi-dynamic wireless charging lies between stationary and dynamic wireless charging, enabling vehicles to receive energy at specific segments of the road or designated parking areas. This approach enhances charging flexibility but is still in the developmental stage regarding its technical maturity [58].

3.1. Stationary Wireless Charging

Stationary wireless charging (SWC) offers a convenient charging experience, allowing vehicles to automatically connect to charging platforms while parked, eliminating the need for manual cable connections [59]. Furthermore, artificial intelligence can intelligently schedule charging times and locations, thereby reducing peak demand for electricity and enhancing charging efficiency [60]. Moreover, the integration of stationary wireless charging systems with autonomous driving enables precise docking of vehicles in parking lots or dedicated charging areas, ensuring both efficiency and safety in the charging process [61]. Ultimately, this integration not only enhances user convenience but also prolongs battery life, reduces operational costs, and contributes to more sustainable transportation solutions. Currently, IPT and CPT technologies represent the most promising advancements in stationary wireless power transmission for EVs [62], as they offer advantages such as high efficiency, enhanced safety, and user convenience. In contrast, technologies like microwave and laser wireless charging may suffer from low efficiency, safety concerns, and high costs, which limit their application in the wireless charging of EVs.

Table 2 summarizes the fundamental characteristics of IPT and CPT couplers. Inductive couplers consist of two coils, L_p and L_s , which transfer power through an intercoupled magnetic field. Inductive couplers are typically characterized by self-inductance as well as mutual inductance (or coupling coefficient k_L) [63]. A typical capacitive coupler comprises four metal plates, P_1 to P_4 , generally represented by six coupling capacitors and mutual capacitance (or coupling coefficient k_C) [64].

Table 2. Fundamental characteristics of IPT and CPT couplers.

Property	Magnetic Coupler	Electric Coupler
Structure		
Coupling		
Self-L/C	L_p, L_s	C_1, C_2
Mutual coupling	L_M	C_M
Coupling coefficient	$k_L = L_M / \sqrt{L_p L_s}$	$k_C = C_M / \sqrt{C_1 C_2}$

Although IPT and CPT differ in their coupling mechanisms and forms, they also share numerous similarities [65]. For instance, in IPT systems, there are four fundamental compensation circuits as follows: series-series (SS) compensation, series-parallel (SP) compensation, parallel-series (PS) compensation, and parallel-parallel (PP) compensation [66–69], as illustrated in Table 3. Similarly, for CPT couplers with the same configuration, four basic compensation circuits have also been proposed, as detailed in Table 4.

Table 3. Four fundamental compensation circuits of IPT.

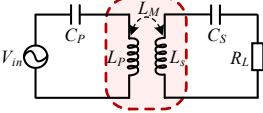
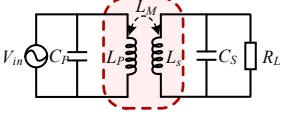
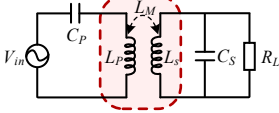
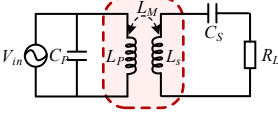
SS-IPT	PP-IPT	SP-IPT	PS-IPT
			
ZPA frequency			
$\omega_0 = \frac{1}{\sqrt{L_p C_p}}$ $= \frac{1}{\sqrt{L_s C_s}}$	$\omega_0 = \frac{1}{\sqrt{L_p C_p (1 - k_L^2)}}$ $= \frac{1}{\sqrt{L_s C_s (1 - k_L^2)}}$	$\omega_0 = \frac{1}{\sqrt{L_p C_p (1 - k_L^2)}}$ $= \frac{1}{\sqrt{L_s C_s}}$	$\omega_0 = \frac{1}{\sqrt{L_p C_p}}$ $= \frac{1}{\sqrt{L_s C_s (1 - k_L^2)}}$
Output property with the voltage source			
$I_{out} = -V_{in} / (j\omega_0 L_M)$	$I_{out} = V_{in} / (j\omega_0 L_M (1/k_L^2 - 1))$	$V_{out} = V_{in} L_s / L_M$	$V_{out} = V_{in} L_M / L_p$

Table 4. Four fundamental compensation circuits of CPT.

SS-CPT	PP-CPT	SP-CPT	PS-CPT
ZPA frequency			
$\omega_0 = \frac{1}{\sqrt{L_1 C_1 (1 - k_c^2)}}$ $= \frac{1}{\sqrt{L_2 C_2 (1 - k_c^2)}}$	$\omega_0 = \frac{1}{\sqrt{L_1 C_1}}$ $= \frac{1}{\sqrt{L_2 C_2}}$	$\omega_0 = \frac{1}{\sqrt{L_1 C_1}}$ $= \frac{1}{\sqrt{L_2 C_2 (1 - k_c^2)}}$	$\omega_0 = \frac{1}{\sqrt{L_1 C_1 (1 - k_c^2)}}$ $= \frac{1}{\sqrt{L_2 C_2}}$
Output property with the voltage source			
$I_{out} = -V_{in} j \omega_0 C_M (1/k_c^2 - 1)$	$I_{out} = V_{in} j \omega_0 C_M$	$V_{out} = V_{in} C_1 / C_M$	$V_{out} = V_{in} C_M / C_2$

In IPT systems, to achieve zero reactive power, only the series-series (SS) compensation topology can fulfill this requirement. Moreover, the resonant frequency of the SS-compensated IPT system is independent of the coupling coefficient, making it the optimal choice for IPT systems [66]. Conversely, in CPT systems, zero reactive power circulation can only be achieved under parallel-parallel (PP) compensation, which similarly does not have its resonant frequency affected by the coupling coefficient [70]. However, the PP-compensation CPT topology is rarely employed in practical applications due to the limitations imposed by the actual input and output voltages on the port voltage of capacitive couplers, resulting in lower power transfer capabilities. Overall, while IPT and CPT systems exhibit similarities, the series and parallel compensation of capacitors in IPT circuits corresponds to the parallel and series compensation of inductors in CPT circuits. Currently, IPT technologies have garnered more extensive research on wireless charging for EVs, as they offer higher transmission power and efficiency compared to CPT systems.

Figure 8 shows a schematic of stationary charging of IPT for EVs. The IEC 61980 standard outlines requirements and guidelines for EV wireless charging systems [71]. The SAE J2954 standard defines various power levels and their corresponding power supply requirements for wireless EV charging systems [72]. Specifically, WPT 1 supports a maximum input power of 3.7 kW, while WPT 2 and WPT 3 provide power levels of 7.7 kW and 11 kW, respectively. WPT 4 supports a power level of up to 22 kW, utilizing a three-phase power supply. Additionally, for heavy-duty applications, the SAE J2954/2 is designed with a power range of 22 to 150 kW [73]. These standards offer flexible charging solutions for different types of EVs, catering to the diverse needs of both light and heavy-duty vehicles, thereby facilitating the widespread adoption of wireless charging technology. Furthermore, Table 5 provides a comprehensive summary of the various power levels for stationary inductive charging systems for EVs.

In terms of economics, Longo et al. estimated the economic viability of wired and wireless charging in Italy and Europe using classical economic indicators [74]. The estimates indicated that in the Italian market, the price of wireless chargers would need to be reduced by 39% compared to their actual value, while in the European market, a reduction of 33% would be necessary for wireless charging to become more economically viable. However, this survey ignores consumer awareness, preferences, and the competitive landscape. A comprehensive cost-benefit analysis, including long-term savings and environmental impact, is also needed. Regulatory support and infrastructure readiness also play a crucial role, and ongoing technological innovations could also change the cost dynamics. These

considerations are critical to developing effective pricing strategies and promoting the widespread adoption of wireless chargers.

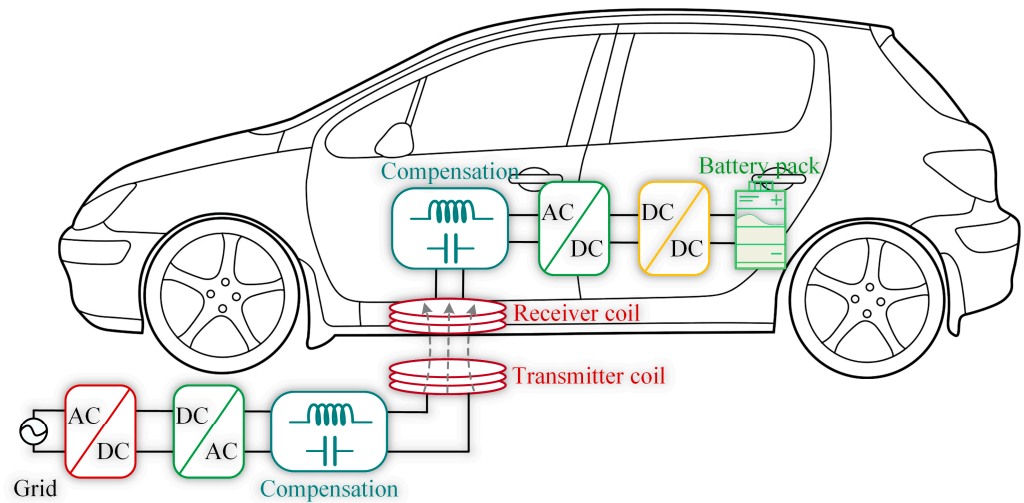


Figure 8. Schematic of stationary wireless charging of IPT for EVs.

Table 5. Summary of the various power levels for stationary inductive charging systems for EVs.

Power (kW)	Frequency (kHz)	Efficiency	Air Gap (mm)	Reference
3	50	90% G2B	200	[75]
3.7	37	91.6% D2D	100	[76]
6	95	95.3% G2B	150	[77]
7.7	85	94.93% D2D	200	[78]
11	85	91.4% D2D	150	[79]
22	100	97% C2C	135	[80]
25	85	91% G2B	210	[81]
50	85	95.8% D2D	10–200	[82]
100	25	97.7% C2C	125	[83]

Note: G2B: grid to battery; C2C: coupler to coupler; D2D: DC to DC.

The evaluation of EV wireless charging technology relies on both internal and external criteria. Internal criteria include metrics such as efficiency, charging speed, alignment tolerance, and user experience, which are critical for assessing the performance and usability of inductive power transfer (IPT) systems. In contrast, external criteria include regulatory standards, market demand, interoperability, infrastructure availability, environmental impact, public perception, technological advancements, economic incentives, and global standards. These factors significantly affect the adoption and acceptance of wireless charging technologies in the broader market environment.

In addition, the importance of international standards, particularly SAE J2954 and IEC 61890 [71,72], for wireless charging of EVs needs to be emphasized. These standards are instrumental in identifying and refining research gaps in IPT technology. They also facilitate the large-scale application of IPT systems by ensuring safety, interoperability, and compliance across various manufacturers and systems. By adhering to these standards, stakeholders can enhance the reliability and efficiency of wireless charging solutions, ultimately promoting broader acceptance and integration within the automotive industry.

3.2. Dynamic Wireless Charging

Despite the gradual maturation of power levels and technology for stationary wireless charging, large-capacity batteries are still required to achieve a higher driving range. Consequently, dynamic wireless charging (DWC) technology, which allows EVs to be charged while in motion, has attracted significant attention from researchers [84–103].

The Korean Advanced Research Institute (KAIST) team initiated the on-line electric vehicle (OLEV) project in 2009 [84], developing multiple generations of products. The power levels were upgraded from 3 kW to 25 kW, and various magnetic coupling mechanisms suitable for dynamic wireless charging were proposed [85]. Other companies have also introduced prototypes for high-power DWC systems. In 2013, the Integrated Infrastructure Solutions (INTIS) team launched a 60 kW DWC system for the 18m electric bus auto tram and a 30 kW DWC system for the Artega electric sports car [86]. INTIS also designed a DWC testing platform capable of transmitting 200 kW of power over a 25 m long track [87]. The PRIMOVE system from Bombardier can provide 250 kW of power to a 30 m long light rail vehicle [88]. As representative research institutions, the Korean Railroad Research Institute (KRRRI) [89] and the IK4-Ikerlan Research Center [90] developed 1 MW and 50 kW prototypes, respectively, for dynamic wireless charging in railway traction systems.

Due to the rapid movement of the transmitting and receiving coils during power transfer in a DWC system, the design and control complexity of the system is significantly increased. Therefore, researchers at universities and other institutions have focused on improving the system's output power fluctuations and stability issues caused by factors such as mutual inductance variations and communication delays. They have addressed these challenges through multiple aspects, including pad configuration [84,91–98], advanced modeling, and control loop optimization [99–103].

Pad configuration, also known as magnetic coupler design, is crucial in DWC systems. It is generally classified into the following two types: elongated rail and multi-coil segmented configurations, as shown in Figure 9a,b, respectively. The rail-based technology route is represented by KAIST, which has developed various generations of prototypes under its OLEV project [85]. Based on the shape of the magnetic core, the transmitting end can be categorized as E-type (1st Gen), U-type (2nd Gen), W-type (3rd Gen), S-type (4th Gen), and I-type (5th Gen) [84,91]. Optimizing the magnetic coupler structure has reduced both manufacturing costs and electromagnetic radiation. The track-based transmitters offer unique advantages for powering multiple vehicles simultaneously, as they simplify design and control by minimizing transmitter switching. Additionally, the magnetic field strength within the track is relatively uniform over a large area, making it easier to control output power fluctuations. However, this approach has drawbacks in light-load conditions (when the number of vehicles is small), as it generates excess electromagnetic fields that result in low system efficiency. Moreover, due to the small coupling coefficient between the tracking transmitter and the vehicle-side receiver coils, the overall efficiency is limited to around 80% [84].

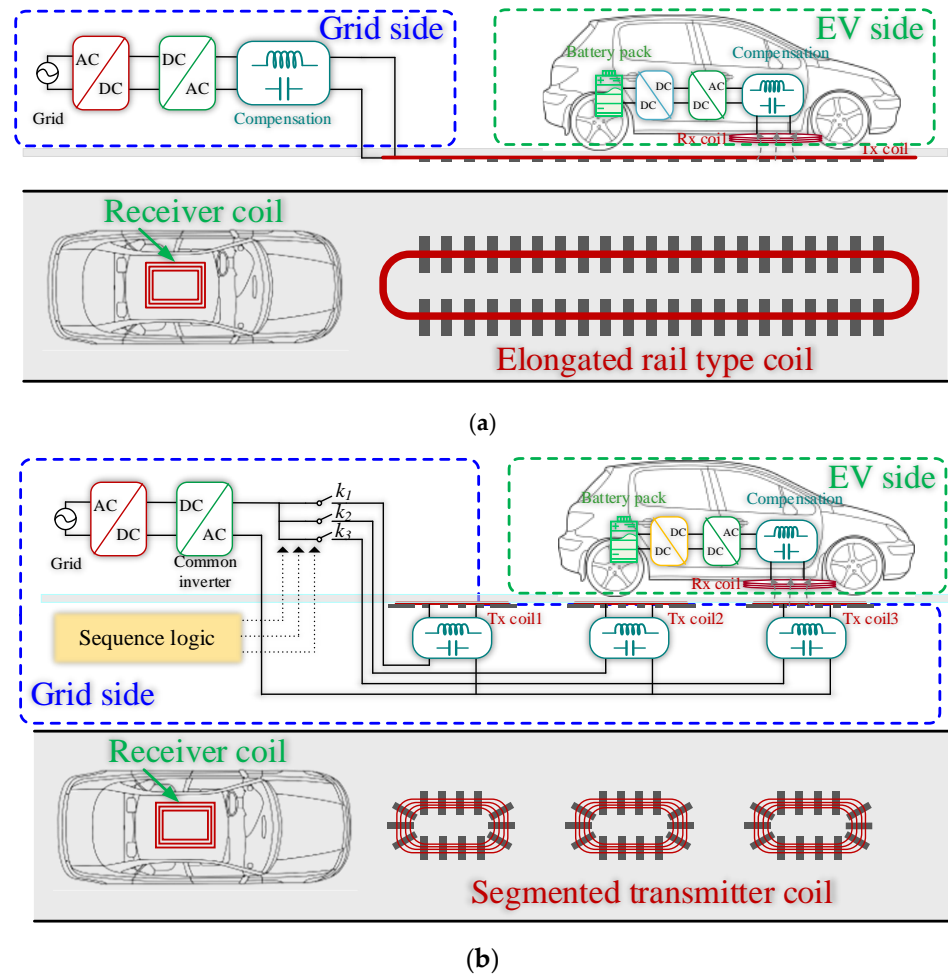


Figure 9. Schematic of DWC for EVs: (a) elongated rail type and (b) segmented transmitter type.

To address the aforementioned issues, many researchers have adopted multiple segmented coils to implement DWC [92–98]. This approach enables the activation of only the transmitter coils in the area covered by the vehicle, thereby reducing excess electromagnetic fields (EMF). For example, a team from Nissan Research Center employed five $1.6 \text{ m} \times 0.3 \text{ m}$ transmitter coils to power a 0.4 m diameter receiver coil, achieving 1 kW DWC with an efficiency of 90% [92]. Similarly, Buja et al. used multiple DD coils on the transmitting end to form a lumped track [93]. They calculated parameters such as the primary coil length and spacing based on the energy required per unit distance of the vehicle. They also discovered that the voltage induced by the movement of the receiving coil could be neglected in the design of the track layout.

To mitigate power fluctuations caused by the magnetic field drop between transmitter segments, Zhang et al. proposed a grouped periodic series spiral coupler to ensure that the receiver is simultaneously coupled with both the preceding and following transmitter coils during coil switching [94]. In [95], an unequal DD configuration was adopted to provide a better power profile and reduce the transmitter coil deployment cost. Tavakoli et al. optimized transmitter coils from the perspective of ground assembly cost and transmission efficiency using a particle swarm optimization algorithm [96], resulting in an optimal pad length of 1.75 m for a 3.7 kW system. Similarly, Chen et al. optimized a proposed two-phase DDQ track considering cost, interoperability, and coupling profile while also reducing the complexity of simulations [97]. Furthermore, Bagchi et al. categorized segmented multi-coil transmitters into three types based on their magnetic field characteristics and highlighted that coil arrangements with alternating magnetic poles along the EV's direction

of motion offer better interoperability, as they can also be used for stationary wireless charging, especially for multiple loads [98].

In addition to optimizing the design of transmitter and receiver pads, the lateral and longitudinal misalignment of the receiver caused by vehicle movement, along with rapid variation in mutual inductance, impose higher demands on system modeling and control. In [99], a 25 kW DWC system was modeled using the generalized state-space averaging method, and a dual-loop controller was designed to regulate primary-side power and current. While primary-side control offers simplicity, it struggles to ensure stable power output on the secondary side at high vehicle speeds. Therefore, receiver-side control has been adopted in [100–102]. In [100] and [101], model predictive control and passivity-based PI control were introduced and compared with traditional PID controllers, demonstrating improved dynamic tracking performance. Zhang et al. addressed disturbances caused by lateral misalignment by modeling longitudinal misalignment and introducing a disturbance observer, significantly enhancing the system's power output robustness.

3.3. Quasi-Dynamic Wireless Charging

Compared to dynamic wireless charging and fully stationary wireless charging, quasi-dynamic wireless charging technology offers distinct advantages in terms of cost, flexibility, and real-time capability [103,104]. It is particularly well-suited for parking scenarios such as intersections and bus stations, providing EVs with more convenient, flexible, and timely charging services [105], as shown in Figure 10.

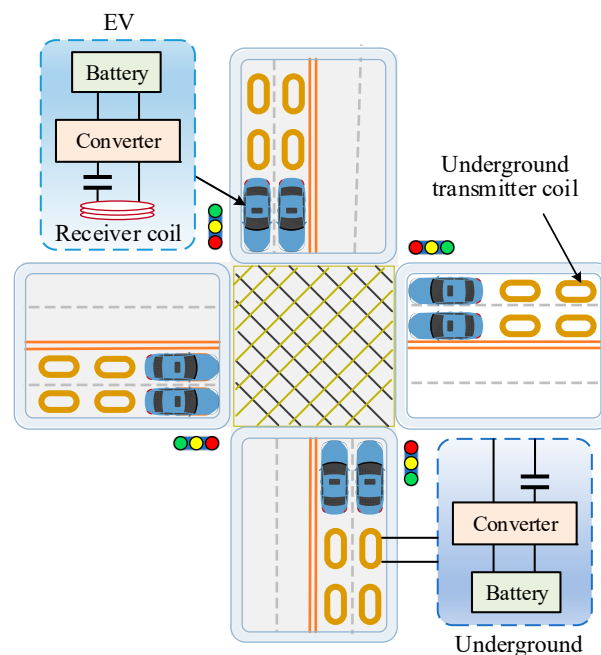


Figure 10. Schematic of quasi-dynamic wireless charging for EVs at intersections.

In dynamic wireless charging, a substantial number of charging facilities must be installed along the route to meet the continuous energy requirements of EVs in motion, which escalates installation and maintenance costs [106]. Conversely, while fully stationary wireless charging does not necessitate numerous charging facilities, its fixed charging points may not adequately accommodate the flexible charging needs of EVs [107]. In contrast, quasi-dynamic wireless charging technology requires the installation of wireless charging facilities only at specific locations, such as traffic intersections or bus stations, significantly reducing costs while fulfilling the charging requirements of EVs during short stops, thus enhancing the practicality and economic viability of charging [108].

Additionally, quasi-dynamic wireless charging technology provides greater flexibility and convenience compared to stationary wireless charging [109]. In scenarios at intersections or bus stations, EVs can recharge during short stops, such as waiting at red lights or for traffic to clear, making effective use of fragmented time to supplement energy and improve travel efficiency. This intelligent charging approach also offers more charging options for EVs, alleviating user anxiety related to charging and enhancing driving convenience.

Furthermore, quasi-dynamic wireless charging technology allows for energy transactions based on real-time traffic conditions and the energy needs of electric vehicles, facilitating bidirectional energy flow [110,111]. Overall, it presents advantages in cost, flexibility, and convenience, offering a more intelligent and efficient charging solution for EVs, which could become a significant development direction in the field of EV charging, promoting their widespread adoption and advancement. However, the application of EV quasi-dynamic wireless charging at intersections and traffic lights faces several challenges, such as the design of equipment layout and coverage, balancing transmission efficiency with charging speed, and considerations regarding safety and electromagnetic radiation [112]. By continuously optimizing and refining technological solutions, this approach can be widely implemented in parking scenarios like intersections, opening up new possibilities for intelligent charging of EVs.

4. Optimization of Wireless Charging Technologies for EVs

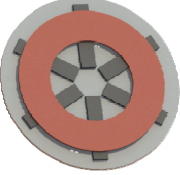
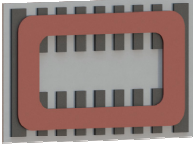

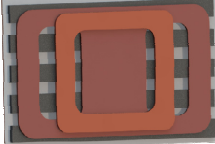

The optimization of WPT technology is crucial for enhancing the performance of wireless charging for EVs. As EVs become more prevalent, the need for efficient and convenient charging solutions has become increasingly urgent. This section will focus on several key areas, including the optimization of coil structures, the optimization of anti-misalignment, the optimization of compensation networks, the optimization of modulation strategies, and the identification of key parameters. These systematic discussions aim to offer valuable insights and practical guidance for the development of wireless charging technologies for EVs.

4.1. Optimization of Coil Structures

In IPT systems, coils play a critical role as the medium for power transfer between the transmitter and receiver. Given the design goal of increasing power transfer per unit volume while increasing frequency, transmitter coil current, and the receiver-side loaded quality factor Q_s can all enhance output power; each comes with limitations. Frequency is constrained by switching losses, current is limited by wire dimensions, system size, and thermal management, and excessively increasing Q_s raises the system's VA rating and complicates tuning. Consequently, optimizing the coil itself is the most direct and effective approach. Table 6 presents common types of coils, which will be discussed in detail.

In [113], it is highlighted that the WPT figure of merit is determined by $k\sqrt{Q_{L1}Q_{L2}}$, where k is the coupling coefficient and Q_{L1} and Q_{L2} are the quality factors of the primary and secondary coils, respectively. IPT coils commonly use Litz wire to mitigate the high-frequency conduction losses caused by skin and proximity effects, yielding a high native Q value in the range of a few hundred. Hence, current coil optimization research primarily focuses on improving coil structure or magnetic material configuration to enhance the coupling coefficient k , increasing misalignment tolerance (to minimize VA growth during misalignment), and adopting self-resonant coils for a more compact and integrated design.

Table 6. Summary of common magnetic couplers for EV charging in the IPT system.

CP	RP	DDP	DDQ Pad	BPP
				
<ul style="list-style-type: none"> • Most common • Easy to fabricate • Poor interoperability • Good power density 	<ul style="list-style-type: none"> • Very common • Easy to fabricate • Suitable for DWPT • Interoperable with CP 	<ul style="list-style-type: none"> • Commonly used on the primary side • Higher horizontal misalignment tolerance 	<ul style="list-style-type: none"> • Commonly used on the secondary side • Hard to fabricate • Interoperable with other pads 	<ul style="list-style-type: none"> • Versatile function • Almost same performance with DDQ • Interoperable with other pads

Magnetic couplers can be categorized based on flux paths into double-sided couplers [114–116] and single-sided couplers [117–122]. Double-sided couplers, often in the form of solenoidal coils, can increase flux height within the same size, thereby improving transmission distance or enhancing offset tolerance [113]. However, they have relatively lower Q values and generate strong horizontal magnetic fields at the ends of the pads, leading to increased stray fields and EMI. Consequently, they may be better suited for wireless charging scenarios with track-type transmitters, such as powering automated guided vehicles (AGVs).

For stationary charging scenarios in electric vehicles, single-sided couplers are a more suitable choice. Common designs include circular pads (CPs) [117], rectangular pads (RPs) [118], double-D pads (DDPs) [119], double-D quadrature (DDQ) pads [120], and bipolar pads (BPPs) [121].

As one of the most common and earliest used coils, CPs and RPs are often equipped with various forms of ferrite underneath to reduce the magnetic reluctance along the flux path and minimize leakage flux. Additionally, aluminum plates are used for magnetic shielding to reduce external interference from the system. In [117], finite element analysis was employed to optimize the efficiency and weight of CPs. To address the issue of significant leakage flux in solenoidal coils, single-sided DD coils with a similar horizontal flux path were proposed [118]. Essentially, a DD coil consists of two rectangular coils wound in opposite directions and connected together. Like solenoidal coils, this flux pipe-shaped magnetic field distribution offers a higher flux height compared to circular coils, improving energy transfer distance. However, DD coils exhibit a coupling null point at a horizontal offset of approximately 34%, significantly limiting their offset tolerance. To address this issue, a quadrature coil decoupled from the DD coil can be introduced, forming the DDQ pad [118,120]. This configuration enhances misalignment tolerance by compensating for the coupling null point and also enhances interoperability with CP coils, allowing for greater compatibility and flexibility in systems that utilize both types of pads.

In [119], Bosshard et al. compared DDP with RP and found that while the anti-misalignment of DD coils is inferior to that of RP, they produce smaller stray fields, making them advantageous in high-power WPT. However, this contradicts the findings in [120], where a multi-objective optimization was performed under identical physical constraints for the following four common magnetic coupling mechanisms: DD transmitter (Tx)-DDQ receiver (Rx), CP (Tx + Rx), RP (Tx + Rx), and DD (Tx + Rx). The study compared their performance in terms of transmission efficiency, power density, and offset tolerance. The

results concluded that CP exhibits the best efficiency and coupling coefficient under the given constraints, requiring the least amount of wire. DD and DDQ, however, demonstrated superior offset tolerance only in specific directions, limiting their overall advantages.

BPP achieves decoupling by partially overlapping two RP coils [121]. This design allows for magnetic field adjustment in both horizontal and vertical directions while reducing complexity and material usage compared to DDQ coils. The characteristics of BPP also make it highly interoperable with other types of coils, enhancing its versatility in various wireless power transfer applications. Similar to the BPP, the Tripolar Pad (TPP) achieves mutual decoupling among three coils [122]. In addition to a higher coupling coefficient compared to CP, the TPP also resists rotational misalignment like CP. In [123], a hexagonal array coil was utilized to provide a more flexible combination and seamless splicing, resulting in a more uniform magnetic flux distribution. To facilitate the selection of a suitable magnetic coupler, Table 6 summarizes the discussed single-sided couplers and highlights their respective characteristics.

Finite Element Analysis (FEA) simulations, known for their precision, are commonly combined with optimization algorithms to improve the performance of magnetic couplers in wireless power transfer systems. Key parameters such as ferrite size, shape, and position [124]; wire thickness and turns [125]; coil-to-core gaps [126]; and shielding plate thickness are optimized to enhance coupling efficiency and offset tolerance [127,128].

For instance, [125] analyzed the trade-offs between coil efficiency and power density, optimizing circular coils using the kQ product (coupling coefficient k and quality factor Q) to identify a Pareto front of design parameters. In [127], a decoupling optimization method for three-coil couplers improved horizontal and vertical offset tolerance by refining coil dimensions and turn counts.

4.2. Optimization of Compensation Network

In IPT, the design of the compensation network is crucial, as different compensation topologies significantly affect the system's efficiency and performance [129]. Factors such as misalignment of the coupling mechanism, frequency deviation, leakage inductance of the transmitting and receiving coils, reactive power circulation, zero phase angle (ZPA) operation, frequency splitting, and soft switching of power electronic devices render the four basic compensation networks inadequate for meeting operational requirements [130,131]. To address the challenges faced by basic compensation networks from a system perspective, several advanced compensation networks have been proposed, including inductor-capacitor-inductor (LCL)-LCL [132], LCL-series (S) [133], LCC-LCC [134], LCC-S [135], LCC-parallel (P) [136], and S-CLC [137], as shown in Figure 11. These higher-order compensation networks aim to enhance performance in IPT systems by mitigating issues related to misalignment, frequency variations, and other operational constraints.

The LCC-LCC high-order compensation network has garnered extensive research due to its ability to enhance power transfer efficiency across a wide range of coupling coefficients and load conditions while also maintaining lower voltage and current stress on the compensation components [138,139]. However, compared to the four basic compensation networks, like SS compensation, the additional compensation capacitors or inductors in high-order circuits can introduce internal resistance, potentially resulting in increased power losses. This can be mitigated by utilizing high-quality (Q) factor capacitors and inductors to reduce copper losses [140]. A high Q value indicates that a component has more reactance and less resistance at a given frequency; it can help to reduce the current strength in the conductor and contributes to the reduction in heat generated by copper losses. In addition, they have a better response at high frequencies, reducing harmonic distortion, improving circuit stability, and ultimately increasing overall energy efficiency.

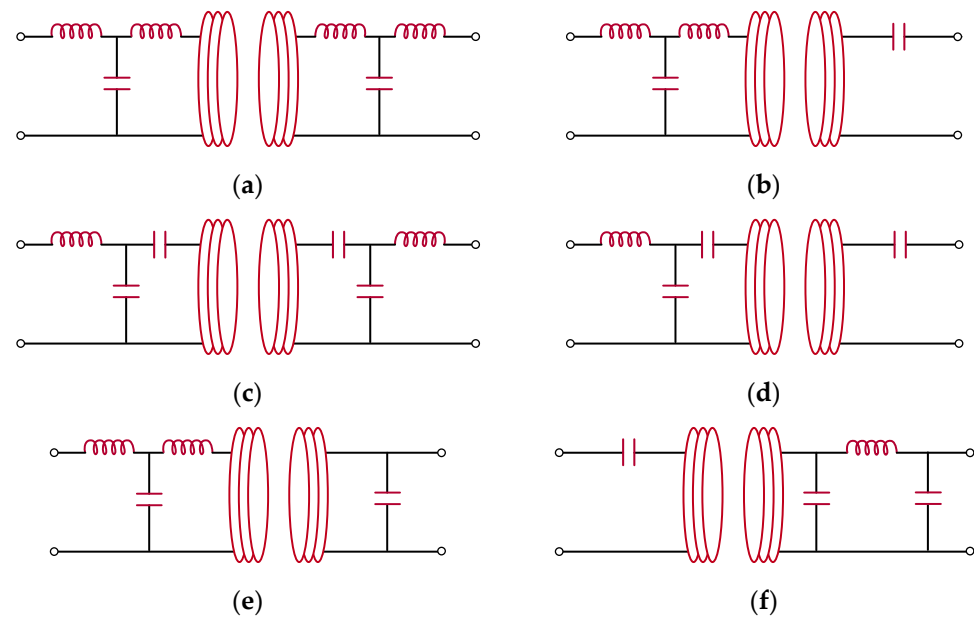


Figure 11. Higher-order compensation networks for IPT systems: (a) LCL-LCL, (b) LCL-S, (c) LCC-LCC, (d) LCC-S, (e) LCC-P, and (f) S-CLC.

Moreover, LCL-LCL and LCC-LCC technologies are strong candidates for wireless charging of EVs, as they enable the current source inverter at the receiver end to work in conjunction with the voltage source inverter at the transmitter end [141–143]. Additionally, achieving zero-voltage switching (ZVS) and soft switching techniques is relatively straightforward within these compensation networks. Notably, the LCC-LCC compensation network can achieve a unit power factor, high efficiency, and reliable operation even under misalignment conditions [144].

Despite the numerous advantages of LCC-LCC compensation, this high-order network inevitably faces challenges related to increased system size and component costs. Nonetheless, its independence from load characteristics, high efficiency, adaptability under misalignment, and ability to reduce inverter current stress make it one of the most used compensation technologies. Various compensation topologies based on LCL compensation, such as LCL-P and LCL-LCL, exhibit characteristics like LCC-LCC. However, using LCL-S under short-circuit conditions at the receiving side may lead to a surge in current, which is undesirable [145]. Table 7 compares basic compensation techniques with various high-order compensation technologies, considering factors such as operating frequency, output power, coupling coefficient, transmission efficiency, and air gap distance. It can be seen that both SS compensation and LCC-LCC compensation can achieve more than 95% efficiency, which is attractive for EV wireless charging.

Table 7. Performance comparison of different compensation networks.

Compensation	Frequency (kHz)	Power Level (kW)	Efficiency	Coupling k_L	Air Gap (mm)
S-S [146]	85	1	95%	0.135	200
S-S [147]	85	3.3	93.1%	0.1	100
S-P [148]	23	2	92%	N/A	100
LCC-LCC [138]	85	1.4	89.78%	0.13	150
LCC-LCC [149]	95	5.6	95.36%	0.14–0.3	150
LCC-LCC [140]	79	7.7	96%	0.18–0.32	200
LCL-LCL [147]	85	3.3	89.5%	0.1	100
LCL-S [150]	140	0.45	93%	0.18–0.32	100

4.3. Optimization of Anti-Misalignment

Misalignment between magnetic couplers refers to deviations in their relative positions from the nominal design position. In EV charging scenarios, this misalignment can occur in three primary directions, as shown in Figure 12, namely, vertical, horizontal, and rotational about the vertical axis. In practice, combinations of these misalignment types are common. For example, in the vertical direction, the distance between the transmitting and receiving pads may vary due to differences in ground clearance across vehicle models. Horizontal and rotational misalignments often arise from drivers parking imprecisely. Regardless of the cause, from a circuit perspective, misalignment introduces perturbations to the following three key parameters: the self-inductances of the primary and secondary coils and their mutual inductance. Therefore, mitigating the impact of these perturbations is central to optimizing anti-misalignment performance.

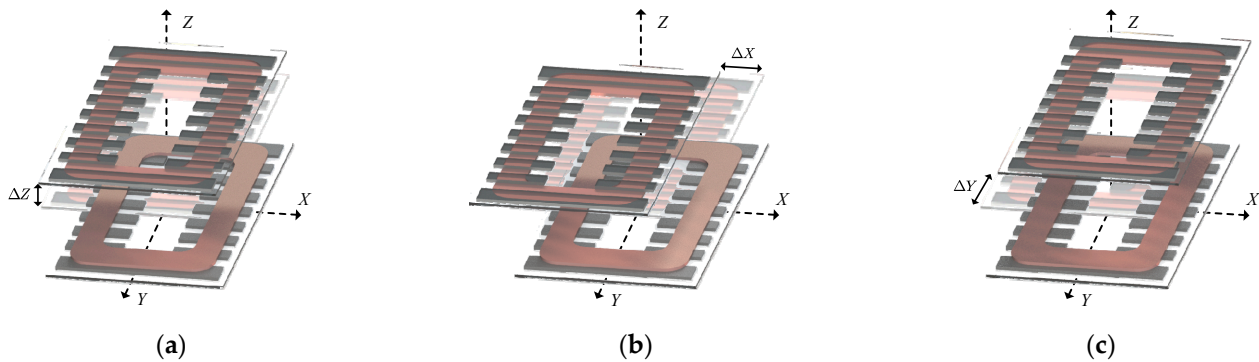


Figure 12. Misalignment conditions in EV wireless charging: (a) vertical direction (Z axis), (b) driving direction (X axis), and (c) transverse direction (Y axis).

To address these challenges, the SAE J2954 standard [72] categorizes vehicle assemblies into the following three vertical ground clearance levels: Z1 (100–150 mm), Z2 (140–210 mm), and Z3 (170–250 mm), which define the required vertical misalignment tolerance. Additionally, the standard specifies allowable horizontal misalignments of (driving direction) and (transverse direction), setting benchmarks for system design and performance.

Improving the anti-misalignment performance of an IPT system is most effectively achieved by optimizing the magnetic coupler, as discussed in the previous section. Under perfectly aligned conditions, CPs deliver the best performance in terms of power density per unit area [120]. However, for misaligned conditions, comparisons of coupler performance across various studies yield inconsistent conclusions due to differing evaluation criteria [118–120,151,152].

For instance, using mutual inductance as the sole metric suggests that the DD-DDQ combination significantly enhances anti-misalignment performance [152]. However, introducing the Q-coil also incurs additional coil losses, weight, receiver pad area, and rectification losses. In [120], it was noted that the anti-misalignment capability of the DDQ pad, in terms of gravimetric power density, showed no substantial improvement over CP. However, this study did not account for vertical misalignment and assumed a fixed air gap, which could affect the conclusions.

Overall, a more comprehensive investigation into anti-misalignment characteristics is necessary. Establishing standardized evaluation metrics would enable consistent assessment of coupler performance and guide engineers in selecting and configuring pads according to various physical constraints during the design phase.

The primary goal of improving magnetic couplers' anti-misalignment performance is to minimize mutual inductance variation during misalignment. Complementary to this, optimizing compensation networks aims to reduce output voltage or power fluctuations

under a given range of coupling coefficient variations. Among the four basic compensation networks (S-S, S-P, P-S, and P-P), only the S-S topology maintains a constant resonant frequency regardless of mutual inductance changes. However, S-S carries the risk of uncontrolled primary-side current under significant misalignment. To address this, Villa et al. analyzed output fluctuation versus coupling factors across various compensation networks (S-S, S-SP, S-CLC, S-LCC, and LCC-S) [153]. The SP-S topology was proposed in [154] to enhance performance under coil misalignment. The results indicated that S-SP, LCC-S, and LCC-LCC topologies exhibit better anti-misalignment performance. Further, [155] conducted a sensitivity analysis of output voltage across multiple topologies and concluded that LCC-LCC offers the best anti-misalignment capability, followed by LCC-S.

In addition to the common compensation networks mentioned above, the series-hybrid topology demonstrated superior anti-misalignment characteristics [156]. Using a DD-DD coil structure, it achieved only a 5% power fluctuation within an X-offset range of -80 to 120 mm, a Y-offset range of ± 160 mm, and a vertical offset range of ± 20 mm. This performance surpasses that of S-S and LCL-LCL topologies, showcasing its robustness in handling misalignment scenarios effectively. Such hybrid topology effectively mitigates the impact of misalignment on power fluctuations because the output characteristics of the two combined topologies exhibit opposite trends in response to misalignment [157].

Reconfigurable circuits are implemented to enhance the anti-misalignment capability. For instance, in [158], the power output exhibits a peak across the coupling coefficient curve. By dynamically switching between full-bridge and half-bridge configurations, impedance matching is achieved, enabling stable power output and high efficiency over a wide range of coupling variations. Similarly, in [159], selecting appropriate compensation networks for different secondary coil positions allows the reuse of the primary coil, improving the system's performance under varying alignment conditions.

Additionally, optimizing the parameters of compensation networks can reduce the system's sensitivity to changes in the coupling coefficient [160,161]. Recently, Wei et al. proposed using self-oscillation control with the S-PS topology to maintain stable power output in the over-coupled region, independent of mutual inductance variations [162]. Compared to other control methods that rely on communication protocols [163,164] or parameter identification techniques [165], this approach demonstrates higher robustness. However, how to ensure system stability and integrate it into practical wireless charging control systems requires further investigation.

4.4. Optimization of System Efficiency

Despite the significant advantages of WPT technology, the efficiency of power transmission remains one of the primary challenges to its promotion and application. In WPT systems, the effective transfer of power not only relies on the rationality of the design but also depends on various factors such as the geometric shape of the coils, the degree of alignment, and the design of the compensation network. Furthermore, minimizing inverter losses is particularly crucial in enhancing the efficiency of WPT systems [166]. While wide-bandgap power devices can somewhat reduce output capacitance and reverse recovery charge, soft-switching techniques remain an effective means to decrease switching losses. As shown in Figure 13, common modulation methods include phase-shift modulation (PSM) [167–169], pulse frequency modulation (PFM) [170,171], and pulse density modulation (PDM) [172,173].

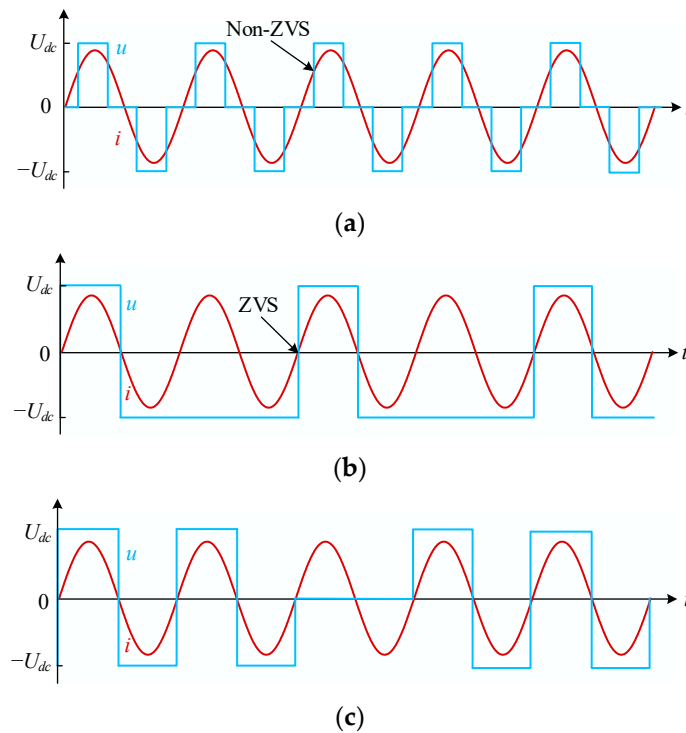


Figure 13. Modulation methods for WPT: (a) phase-shift modulation (PSM), (b) pulse frequency modulation (PFM), and (c) pulse density modulation (PDM).

The technique of adjusting the output pulse width by altering the phase difference of the triggering signals of the two arms of the inverter, without changing the pulse frequency, is known as phase-shift modulation (PSM), as shown in Figure 13a [167]. This phase difference is referred to as the phase-shift angle, while the width of the output pulse is termed the duty cycle. There exists a complementary relationship between the phase-shift angle and the duty cycle, that is, as the phase-shift angle increases, the duty cycle decreases, resulting in a reduction in both the output pulse width and the fundamental effective value; conversely, a decrease in the phase-shift angle leads to an increase in the duty cycle, along with an increase in the output pulse width and fundamental effective value [168]. The duty cycle can vary continuously between 0 and 1, indicating that PSM modulation enables a full range of seamless adjustment. However, adjusting the duty cycle may incur hard-switching losses, adversely impacting system efficiency. Although complex zero-voltage switching (ZVS) angle control can facilitate soft switching, it also adds to the complexity of the system [169].

Pulse frequency modulation (PFM) is a method for controlling the effective value of the inverter output by varying the proportions of voltage pulses at different frequencies, characterized by a constant pulse width duty cycle, as shown in Figure 13b [170]. The advantage of PFM lies in its simplicity for achieving wide-range soft switching and reducing the switching frequency of the inverter [171]. Nonetheless, the overall efficiency of the system may decline under light load conditions. A method combining key control modulation and PFM for maximum efficiency tracking was proposed in [174], although this approach can lead to significant output current ripple and disruption issues.

Half-wave PFM was first proposed in [175,176] and applied in self-oscillating WPT systems to ensure reliable ZVS output power regulation. Additionally, Wang et al. further explore the application of PFM in high-order compensation topologies for wireless charging [177]. However, these PFM methods exhibit limited flexibility; for specific modulation coefficients, the number of mixed-frequency pulse sequences must be predetermined. To address this issue, an improved PFM based on Σ - Δ modulators has been proposed, al-

lowing for direct frequency changes through varying sampling periods, thus facilitating seamless pulse instruction modulation [178]. Guo et al. expanded the application of Σ - Δ modulators to three-level inverters while also considering mid-point balancing, despite the complexity of implementation [179].

Pulse density control is a method for regulating the effective output voltage by adjusting the number of pulses within each modulation cycle (i.e., pulse density), without altering the pulse frequency or duty cycle, as shown in Figure 13c [180]. A significant issue with conventional pulse density modulation (PDM) is the severe oscillation of the inverter's output current, particularly at lower pulse densities [181].

To address this, enhanced PDM (EPDM) and similar modulation schemes have been proposed to further reduce output current ripple in full-bridge inverters [182]. Li et al. introduce a PDM strategy for a WPT system based on a dual-sided half-bridge converter, aiming to achieve ZVS and maximum power tracking by adjusting pulse density to regulate output power [183]. However, both coupling and load conditions may affect the soft switching performance of the PDM-WPT system. To ensure soft switching under various operating conditions, a PDM full-bridge converter equipped with ZVS branches between switching nodes was proposed [184], though this approach has the drawback of modifying the inverter topology and narrowing the modulation range.

To resolve these issues, a low-order harmonic, full-range, rapid PDM strategy was developed [185]. Additionally, improved PDM methods reduce output power fluctuations by switching the inverter from full-bridge mode to half-bridge mode [186,187]. Nevertheless, PDM-WPT systems require additional auxiliary circuits to alter the current frequency to maintain soft switching. To mitigate current oscillations, conditional pulse density modulation and hybrid modulation methods have been proposed, yielding complementary effects [188,189]. Recently, Tang et al. introduced step density modulation, which regulates output power through varying step densities, producing fewer output current harmonics compared to traditional PDM [190]. Furthermore, a pulse magnitude modulation combined with multi-level converters has been proposed, further expanding the modulation strategies for WPT systems [191].

4.5. Key-Parameters Identification

Parameter identification in WPT systems is a critical process for optimizing system performance. Based on the identification targets, parameter identification techniques can be classified into the following three categories: mutual inductance identification, simultaneous identification of load and mutual inductance, and multi-parameter joint identification techniques.

Mutual inductance identification plays a vital role in wireless charging systems, as recognizing it aids in determining the relative position of coils and assessing system conditions. The output impedance characteristics of the inverter in the frequency domain were analyzed in [192], establishing the relationship between mutual inductance and inverter output impedance. This is achieved through the measurement of output voltage, current, and phase information from the inverter, facilitating the estimation of mutual inductance parameters. In addition, a time-domain model of a WPT system based on SS compensation topology is derived [193], resulting in a fourth-order time-domain differential equation that includes mutual inductance parameters. Similar to the previous study, this method estimates mutual inductance using inverter output voltage, current, and phase information. These methods require zero-crossing detection circuits or discrete Fourier transforms to obtain fundamental phase information, imposing stringent requirements on detection circuitry or digital signal processors, and they necessitate prior knowledge of load parameters, making them unsuitable for systems with varying loads.

To identify mutual inductance parameters under unknown load conditions, Yang et al. propose a method involving hardware switching to short-circuit the lower bridge arm of a controllable rectifier bridge and use frequency sweeping to estimate the coupling coefficient [194]. Wang et al. employ a soft-start process to estimate mutual inductance by obtaining the effective values of inverter voltage and current at low output voltage levels [195]. These methods do not require consideration of load parameters and are suitable for identification before normal operation. Additionally, mutual inductance identification methods utilizing information from fundamental and higher harmonic components were explored [196,197], though attention must be paid to the errors introduced by higher harmonics.

In practical applications, WPT systems often encounter the challenge of simultaneous changes in mutual inductance and load parameters. To address this, researchers have proposed various solutions for the concurrent estimation of load and mutual inductance. Dai et al. utilize radio frequency-link wireless communication to transmit load information from the receiving end to the transmitting end, integrating inverter data to identify multiple mutual inductance parameters [198]. Additionally, some methods based on auxiliary capacitors and supplementary inverters to achieve mutual inductance and load identification were proposed [199,200]; while effective, these approaches increase system complexity. Conversely, Su et al. proposed a solution that requires no additional circuitry, utilizing frequency control to operate the inverter in a ZPA state [201], thereby collecting voltage and current data for parameter identification. Dai et al. employ pulse density modulation to generate inter-harmonics, analyzing related signals to identify mutual inductance and load [202]. These studies provide new insights into enhancing the flexibility and efficiency of WPT systems.

The scope of multi-parameter joint identification has expanded to encompass various parameters, including coil self-inductance, resonant capacitance, and battery status, to meet diverse application needs and enhance system reliability. A multi-parameter joint identification method based on DC input current and phase angle, successfully identifying battery voltage, charging current, and equivalent load impedance of the system, was proposed [203]. This method quantitatively describes the relationship between system characteristics and parameters through linear superposition, utilizing easily obtainable data for parameter estimation.

Further, Guo et al. leverage the quantified relationship of the rectifier bridge input impedance to estimate the state of charge (SOC) of the battery [204]. However, these methods primarily rely on offline data analysis without considering variations in coil position, necessitating optimization for more complex application scenarios. Building on this foundation, Wang et al. introduce an online real-time identification algorithm [205], employing higher-order implicit functions to represent parameter relationships and integrating an improved least-mean-square adaptive filter to achieve rapid online identification. Addressing variations in coil self-inductance, an optimization method for the identification of bilateral coil self-inductance and mutual inductance based on variable switched capacitors was proposed in [206]. These studies provide effective solutions for parameter identification of WPT systems in complex environments.

5. Discussion

5.1. Development Trends

The advancement of WPT technology for EVs operating at high power levels is indeed a pivotal area of research and development. This technology aims to provide efficient, convenient, and rapid charging solutions that can enhance the EV charging experience and promote broader adoption of EVs. High-power WPT systems are focused on maximizing efficiency during the power transfer process. Innovations in resonant inductive couplers,

such as optimized coil design and placement, play a crucial role in reducing energy losses and improving overall system performance.

DWC represents a significant advancement in WPT technology, allowing charging while vehicles are in motion. Recent developments have aimed at enhancing power levels, system efficiency, and stability, with innovations in magnetic coupler designs, such as elongated rail and segmented coil configurations, reducing electromagnetic interference and improving energy transfer. Advanced modeling techniques and control strategies are also being adopted to tackle challenges like misalignment. Future efforts will likely emphasize optimizing system costs, interoperability, and integration with emerging technologies to further improve the practicality and scalability of DWC systems.

Addressing misalignment in WPT systems is critical for stable and efficient charging. Current trends focus on optimizing magnetic coupler designs and enhancing system adaptability through compensation networks and reconfigurable circuits. Simplified control strategies improve robustness by minimizing reliance on complex communication protocols. Future study will prioritize practical integration and standardization of evaluation metrics.

Parameter identification in WPT systems faces challenges related to accuracy and environmental adaptability. Current methods are often limited to specific topologies and susceptible to interference. Future research should concentrate on multi-parameter joint identification to enhance system reliability and efficiency. Developing adaptable algorithms and integrating real-time data processing will be crucial for dynamic adjustments. Strengthening interdisciplinary collaboration across fields like artificial intelligence and communication technologies will foster innovative solutions to the challenges faced by WPT systems [207–211]. Accurate and real-time parameter identification will be essential for optimizing WPT performance in increasingly complex application scenarios.

Furthermore, it is important to recognize the critical role of wireless communications and protocols in the wireless charging of electric vehicles. Effective communication is essential for ensuring interoperability among various EV models and charging stations, which is vital for the widespread adoption of this technology. Furthermore, robust communication systems provide real-time data regarding charging status, battery health, and potential faults, thereby enhancing safety and optimizing charging efficiency. Standards such as IEC 61980 offer guidelines for these communication protocols, underscoring their importance in creating a seamless user experience and supporting the transition to electric mobility.

5.2. Limitations

Many existing WPT systems provide limited power transfer capabilities, which may fall short of meeting the rapid charging requirements of EVs. Although technology continues to advance, current systems may struggle to deliver the high power levels necessary for quick charging, resulting in longer wait times for users. With the development of superconducting technology, the active development of superconducting WPT will bring the possibility of high-power wireless charging [212,213].

Furthermore, high-power WPT systems generate substantial heat during operation, presenting challenges for thermal management. This is because increased charging power leads to heat buildup, which affects charging efficiency and safety. Excessive heat can adversely affect the performance and longevity of electronic components, potentially leading to failures [213]. Inadequate thermal management can diminish the efficiency of power transfer and increase the risk of overheating. Therefore, effective cooling solutions, such as active cooling systems, high thermal conductivity materials, and optimized design of couplers [214,215], are needed to ensure that the system maintains appropriate operating temperatures during high power transfer, thereby improving overall efficiency and reliability.

Additionally, concerns regarding electromagnetic interference and safety must be addressed. The intense electromagnetic fields generated by high-power WPT systems can interfere with nearby electronic devices, including sensitive electronic components in electric vehicles and surrounding infrastructure, affecting communication systems and vehicle controls, potentially leading to malfunctions or degraded performance of the EVs [216]. Therefore, effective shielding and filtering techniques must be employed in the design of WPT systems to mitigate the effects of electromagnetic interference [217]. To resolve these issues, comprehensive testing and adherence to safety standards are essential to ensure that high-power WPT systems do not cause harmful interference or safety hazards during charging. Moreover, prolonged exposure to strong electromagnetic fields raises safety concerns [218]. Ongoing research aims to understand the potential health impacts of such exposure, including risks associated with long-term use [219,220]. Advanced shielding technologies may be necessary to minimize interference and ensure safety, which can further increase system complexity and costs, impacting the overall design.

6. Conclusions

The advancement of WPT technology represents a significant breakthrough in the realm of EV charging. Among many WPT technologies, the power transfer capability of CPT currently makes it difficult to meet the demand for wireless charging of EVs, and its complex coupling mechanism limits its applicability in the dynamic charging of EVs. Far-field WPT can utilize microwave or laser technology to achieve energy transmission over longer distances, but they suffer from lower efficiency and higher costs, making them less practical for widespread use in EV charging applications. In contrast, IPT emerges as the most promising EV charging technology due to its relatively large transmission power, high efficiency, and anti-misalignment ability. This paper highlights the theoretical foundations, diverse implementation strategies, and optimization techniques that support the development of IPT. Despite commendable progress, several limitations persist, including power losses, high power transfer, EMI interference, safety concerns, and the inherent complexity of system designs, all of which may hinder its widespread application. Future research must prioritize overcoming these obstacles by exploring innovative methods that can enhance the practicality and performance of wireless charging technology. This encompasses investigating advanced coil designs, improving energy transfer efficiency, and developing robust safety mechanisms to ensure user confidence. With the advent of an era characterized by smart cities and autonomous EVs, wireless charging will be essential in supporting the ecosystem necessary for the flourishing of electric mobility, aiding in the establishment of a more environmentally friendly and efficient transportation system, in alignment with global efforts to reduce carbon emissions and promote urban sustainability.

Author Contributions: Z.X.: conceptualization, writing—original draft preparation, methodology, investigation. W.L.: conceptualization, methodology, writing—review and editing, investigation. C.L.: conceptualization, methodology, investigation, writing—original draft preparation. K.T.C. conceptualization, supervision, funding acquisition, project administration, writing—review and editing. All authors have read and agreed to the published version of the manuscript.

Funding: This study was partially supported by two grants from the Hong Kong Research Grants Council, Hong Kong Special Administrative Region, China, under Project No. T23-701/20-R and Project No. 17206222, and partially supported by a grant from The Hong Kong Polytechnic University, under Project No. P0048560.

Data Availability Statement: No new data were created or analyzed in this study. Data sharing is not applicable to this article.

Conflicts of Interest: The authors declare no conflicts of interest.

References

1. IEA. Global EV Outlook 2024 [EB/OL]. Available online: <https://www.iea.org/reports/global-ev-outlook-2024> (accessed on 1 April 2024).
2. Lukic, S.; Pantic, Z. Cutting the cord: Static and dynamic inductive wireless charging of electric vehicles. *IEEE Electrific. Mag.* **2013**, *1*, 57–64. [CrossRef]
3. Liu, W.; Chau, K.T.; Tian, X.; Wang, H.; Hua, Z. Smart wireless power transfer—Opportunities and challenges. *Renew. Sust. Energ. Rev.* **2023**, *180*, 113298. [CrossRef]
4. Zhang, Z.; Pang, H. Continuously adjustable capacitor for multiple pickup wireless power transfer under single-power-induced energy field. *IEEE Trans. Ind. Electron.* **2020**, *67*, 6418–6427. [CrossRef]
5. Xue, Z.; Chau, K.T.; Liu, W.; Fan, Y.; Hou, Y. Wireless power, drive, and data transfer for ultrasonic motors. *IEEE Trans. Ind. Electron.* **2025**, *72*, 134–144. [CrossRef]
6. Hui, S.Y.R.; Zhong, W.; Lee, C.K. A critical review of recent progress in mid-range wireless power transfer. *IEEE Trans. Power Electron.* **2014**, *29*, 4500–4511. [CrossRef]
7. Prasad, D.V.; Lande, V.S.; Bornare, A.P.; Waghmare, P.B.; Sujith, M. Dynamic wireless charging system for electric vehicles. In Proceedings of the 2024 8th International Conference on Inventive Systems and Control (ICISC), Coimbatore, India, 29–30 July 2024; pp. 608–612.
8. Moisello, E.; Liotta, A.; Malcovati, P.; Bonizzoni, E. Recent trends and challenges in near-field wireless power transfer systems. *IEEE Open J. Solid-State Circuits Soc.* **2023**, *3*, 197–213. [CrossRef]
9. Tavakoli, R.; Pantic, Z. DC modeling of an LCC resonant compensation network in wireless power transfer systems. In Proceedings of the 2018 IEEE Energy Conversion Congress and Exposition (ECCE), Portland, OR, USA, 23–27 September 2018; pp. 6187–6193.
10. Rasekh, N.; Kavianpour, J.; Mirsalim, M. A novel integration method for a bipolar receiver pad using LCC compensation topology for wireless power transfer. *IEEE Trans. Veh. Technol.* **2018**, *67*, 7419–7428. [CrossRef]
11. Ahmad, A.; Alam, M.S.; Chabaan, R. A comprehensive review of wireless charging technologies for electric vehicles. *IEEE Trans. Transport. Electrific.* **2018**, *4*, 38–63. [CrossRef]
12. Ahmed, M.M.; Enany, M.A.; Shaier, A.A.; Bawayan, H.M.; Hussien, S.A. An extensive overview of inductive charging technologies for stationary and in-motion electric vehicles. *IEEE Access* **2024**, *12*, 69875–69894. [CrossRef]
13. Gao, X.; Liu, C.; Zhou, H.; Hu, W.; Huang, Y.; Xiao, Y.; Lei, Z.; Chen, J. Design and analysis of a new hybrid wireless power transfer system with a space-saving coupler structure. *IEEE Trans. Power Electron.* **2021**, *36*, 5069–5081. [CrossRef]
14. Rodriguez, J.I.; Jackson, D.K.; Leeb, S.B. Capability analysis for an inductively coupled power transfer system. In Proceedings of the COMPEL 2000. 7th Workshop on Computers in Power Electronics. Proceedings (Cat. No.00TH8535), Blacksburg, VA, USA, 16–18 July 2000; pp. 59–63.
15. Kurs, A.; Karalis, A.; Moffatt, R.; Joannopoulos, J.D.; Fisher, P.; Soljačić, M. Wireless power transfer via strongly coupled magnetic resonances. *Science* **2007**, *317*, 83–86. [CrossRef] [PubMed]
16. Mohammad, M.; Wodajo, E.; Choi, S.; Elbuluk, M. Modeling and design of passive shield to limit EMF emission and to minimize shield loss in unipolar wireless charging system for EV. *IEEE Trans. Power Electron.* **2019**, *34*, 12235–12245. [CrossRef]
17. Shin, J.; Shin, S.; Kim, Y.; Ahn, S.; Lee, S.; Jung, G.; Jeon, S.-J.; Cho, D.-H. Design and implementation of shaped magnetic-resonance-based wireless power transfer system for roadway-powered moving electric vehicles. *IEEE Trans. Ind. Electron.* **2014**, *61*, 1179–1192. [CrossRef]
18. Sakamoto, H.; Harada, K.; Washimiya, S.; Takehara, K.; Matsuo, Y.; Nakao, F. Large air-gap coupler for inductive charger [for electric vehicles]. *IEEE Trans. Magn.* **1999**, *35*, 3526–3528. [CrossRef]
19. Wang, C.-S.; Covic, G.A.; Stielau, O.H. Power transfer capability and bifurcation phenomena of loosely coupled inductive power transfer systems. *IEEE Trans. Ind. Electron.* **2004**, *51*, 148–157. [CrossRef]
20. Liu, W.; Placke, T.; Chau, K.T. Overview of batteries and battery management for electric vehicles. *Energy Rep.* **2022**, *8*, 4058–4084. [CrossRef]
21. Wang, C.-S.; Stielau, O.H.; Covic, G.A. Load models and their application in the design of loosely coupled inductive power transfer systems. In Proceedings of the PowerCon 2000. 2000 International Conference on Power System Technology. Proceedings (Cat. No.00EX409), Perth, WA, Australia, 4–7 December 2000; Volume 2, pp. 1053–1058.
22. Stielau, O.H.; Covic, G.A. Design of loosely coupled inductive power transfer systems. In Proceedings of the PowerCon 2000. 2000 International Conference on Power System Technology. Proceedings (Cat. No.00EX409), Perth, WA, Australia, 4–7 December 2000; Volume 1, pp. 85–90.
23. Mizuno, T.; Yachi, S.; Kamiya, A.; Yamamoto, D. Improvement in efficiency of wireless power transfer of magnetic resonant coupling using magnetoplated wire. *IEEE Trans. Magn.* **2011**, *47*, 4445–4448. [CrossRef]
24. Kim, J.; Kim, J.; Kong, S.; Kim, H.; Suh, I.S.; Suh, N.P.; Cho, D.H.; Kim, J.; Ahn, S. Coil design and shielding methods for a magnetic resonant wireless power transfer system. *Proc. IEEE* **2013**, *101*, 1332–1342. [CrossRef]

25. Lee, J.; Lee, K. Effects of number of relays on achievable efficiency of magnetic resonant wireless power transfer. *IEEE Trans. Power Electron.* **2020**, *35*, 6697–6700. [[CrossRef](#)]
26. Pang, H.; Liu, W.; Xue, Z.; Hou, Y.; Chan, C.C. Load-independent dual-frequency constant-current and constant-voltage wireless power transfer system for multiple pickups. In Proceedings of the 2024 IEEE Wireless Power Technology Conference and Expo (WPTCE), Kyoto, Japan, 8–11 May 2024; pp. 641–645.
27. Oh, S.J.; Khan, D.; Jang, B.G.; Basim, M.; Asif, M.; Ali, I.; Pu, Y.; Yoo, S.S.; Lee, M.; Hwang, K.C.; et al. A 15-W quadruple-mode reconfigurable bidirectional wireless power transceiver with 95% system efficiency for wireless charging applications. *IEEE Trans. Power Electron.* **2021**, *36*, 3814–3827. [[CrossRef](#)]
28. Foote, A.; Asa, E.; Onar, O. Thermal integration of a high power polyphase inductive coil assembly. In Proceedings of the 2024 IEEE Transportation Electrification Conference and Expo (ITEC), Chicago, IL, USA, 19–21 June 2024; pp. 1–5.
29. Han, W.; Chau, K.T.; Jiang, C.; Liu, W.; Lam, W.H. Design and analysis of quasi-omnidirectional dynamic wireless power transfer for fly-and-charge. *IEEE Trans. Magn.* **2019**, *55*, 8001709. [[CrossRef](#)]
30. Gu, W.; Qiu, D.; Shu, X.; Zhang, B.; Xiao, W.; Chen, Y. A constant output capacitive wireless power transfer system based on parity-time symmetric. *IEEE Trans. Circuits Syst. II Exp. Briefs* **2023**, *70*, 2585–2589. [[CrossRef](#)]
31. Luo, B.; Long, T.; Guo, L.; Dai, R.; Mai, R.; He, Z. Analysis and design of inductive and capacitive hybrid wireless power transfer system for railway application. *IEEE Trans. Ind. Appl.* **2020**, *56*, 3034–3042. [[CrossRef](#)]
32. Xue, Z.; Chau, K.T.; Liu, W.; Hua, Z. Magnetic-free wireless self-direct drive motor system for biomedical applications with high-robustness. *IEEE Trans. Power Electron.* **2024**, *39*, 2882–2891. [[CrossRef](#)]
33. Dai, J.; Ludois, D.C. A survey of wireless power transfer and a critical comparison of inductive and capacitive coupling for small gap applications. *IEEE Trans. Power Electron.* **2015**, *30*, 6017–6029. [[CrossRef](#)]
34. Lu, F.; Zhang, H.; Hofmann, H.; Mi, C. A double-sided LCLC-compensated capacitive power transfer system for electric vehicle charging. *IEEE Trans. Power Electron.* **2015**, *30*, 6011–6014. [[CrossRef](#)]
35. Sinha, S.; Regensburger, B.; Doubleday, K.; Kumar, A.; Pervaiz, S.; Afridi, K.K. High-power-transfer-density capacitive wireless power transfer system for electric vehicle charging. In Proceedings of the 2017 IEEE Energy Conversion Congress and Exposition (ECCE), Cincinnati, OH, USA, 1–5 October 2017; pp. 967–974.
36. Regensburger, B.; Kumar, A.; Sinha, S.; Afridi, K. High performance 13.56-MHz large air-gap capacitive wireless power transfer system for electric vehicle charging. In Proceedings of the IEEE 19th Workshop Control Modeling for Power Electron (COMPEL), Padua, Italy, 25–28 June 2018; pp. 1–4.
37. Choi, J.; Tsukiyama, D.; Tsuruda, Y.; Rivas, J. 13.56 MHz 1.3 kW resonant converter with GaN FET for wireless power transfer. In Proceedings of the 2015 IEEE Wireless Power Transfer Conference (WPTC), Boulder, CO, USA, 13–15 May 2015; pp. 1–4.
38. Choi, J.; Tsukiyama, D.; Rivas, J. Comparison of SiC and eGaN devices in a 6.78 MHz 2.2 kW resonant inverter for wireless power transfer. In Proceedings of the 2016 IEEE Energy Conversion Congress and Exposition (ECCE), Milwaukee, WI, USA, 18–22 September 2016; pp. 1–6.
39. Xue, Z.; Chau, K.T.; Liu, W.; Ching, T.W. Design analysis, and implementation of wireless traveling-wave ultrasonic motors. *IEEE Trans. Power Electron.* **2024**, *39*, 4601–4611. [[CrossRef](#)]
40. Gao, X.; Zhou, H.; Hu, W.; Deng, Q.; Liu, G.; Lai, J. Capacitive power transfer through virtual self-capacitance route. *IET Power Electron.* **2018**, *11*, 1110–1118. [[CrossRef](#)]
41. Lu, F.; Zhang, H.; Mi, C. A two-plate capacitive wireless power transfer system for electric vehicle charging applications. *IEEE Trans. Power Electron.* **2018**, *33*, 964–969. [[CrossRef](#)]
42. Zou, L.J.; Zhu, Q.; Van Neste, C.W.; Hu, A.P. Modeling single wire capacitive power transfer system with strong coupling to ground. *IEEE J. Emerg. Sel. Topics Power Electron.* **2021**, *9*, 2295–2302. [[CrossRef](#)]
43. Liu, Z.; Su, Y.; Hu, H.; Deng, Z.; Deng, R. Research on transfer mechanism and power improvement technology of the SCC-WPT system. *IEEE Trans. Power Electron.* **2023**, *38*, 1324–1335. [[CrossRef](#)]
44. Garnica, J.; Chinga, R.A.; Lin, J. Wireless power transmission: From far field to near field. *Proc. IEEE* **2013**, *101*, 1321–1331. [[CrossRef](#)]
45. Brown, W.C. The history of power transmission by radio waves. *IEEE Trans. Microw. Theory Techn.* **1984**, *32*, 1230–1242. [[CrossRef](#)]
46. Shinohara, N. Beam efficiency of wireless power transmission via radio waves from short range to long range. *J. Korean Inst. Electromagn. Eng. Sci.* **2010**, *10*, 4–10. [[CrossRef](#)]
47. Matsumoto, H. Research on solar power satellites and microwave power transmission in Japan. *IEEE Microw. Mag.* **2002**, *3*, 36–45. [[CrossRef](#)]
48. Jin, K.; Zhou, W. Wireless laser power transmission: A review of recent progress. *IEEE Trans. Power Electron.* **2019**, *34*, 3842–3859. [[CrossRef](#)]
49. Luo, B.; Wang, J.; Yang, Y.; Lan, J.; Liu, Y. Evaluation and enhancement of laser power transfer efficiency in the presence of atmospheric turbulence. *IEEE J. Photovolt.* **2024**, *14*, 466–472. [[CrossRef](#)]

50. Chen, Y.; Mou, Z.; Wang, J.; Zhu, L.; Gou, Y.; Sun, Z. 808 nm laser power converters for simultaneous wireless information and power transfer. *IEEE J. Photovolt.* **2024**, *14*, 890–900. [\[CrossRef\]](#)
51. Ho, S.L.; Wang, J.; Fu, W.N.; Sun, M. A comparative study between novel witrlicity and traditional inductive magnetic coupling in wireless charging. *IEEE Trans. Magn.* **2011**, *47*, 1522–1525. [\[CrossRef\]](#)
52. Li, S.; Chau, K.T.; Liu, W.; Liu, C.; Lee, C.K. Design and control of wireless hybrid stepper motor system. *IEEE Trans. Power Electron.* **2024**, *39*, 10518–10531. [\[CrossRef\]](#)
53. Hua, Z.; Chau, K.T.; Liu, W.; Tian, X.; Pang, H. Autonomous pulse frequency modulation for wireless battery charging with zero-voltage switching. *IEEE Trans. Ind. Electron.* **2023**, *70*, 8959–8969. [\[CrossRef\]](#)
54. Shinohara, N.; Kubo, Y.; Tonomura, H. Wireless charging for electric vehicle with microwaves. In Proceedings of the 2013 3rd International Electric Drives Production Conference (EDPC), Nuremberg, Germany, 29–30 October 2013; pp. 1–4.
55. Vincent, D.; Huynh, P.S.; Azeez, N.A.; Patnaik, L.; Williamson, S.S. Evolution of hybrid inductive and capacitive AC links for wireless EV charging—A comparative overview. *IEEE Trans. Transp. Electrification.* **2019**, *5*, 1060–1077. [\[CrossRef\]](#)
56. Shahin, A.; Abdelaziz, A.Y.; Houari, A.; Nahid-Mobarakeh, B.; Pierfederici, S.; Deng, F.; Abulanwar, S. A comprehensive analysis: Integrating renewable energy sources with wire/wireless EV charging systems for green mobility. *IEEE Access* **2024**, *12*, 140527–140555. [\[CrossRef\]](#)
57. Mahesh, A.; Chokkalingam, B.; Mihet-Popa, L. Inductive wireless power transfer charging for electric vehicles—A review. *IEEE Access* **2021**, *9*, 137667–137713. [\[CrossRef\]](#)
58. Mohamed, N.; Aymen, F.; Alharbi, T.E.A.; El-Bayeh, C.Z.; Lassaad, S.; Ghoneim, S.S.M.; Eicker, U. A comprehensive analysis of wireless charging systems for electric vehicles. *IEEE Access* **2022**, *10*, 43865–43881. [\[CrossRef\]](#)
59. Tenllado, I.C.; Cabrera, A.T.; Lin, Z. Simultaneous wireless power and data transfer for electric vehicle charging: A review. *IEEE Trans. Transp. Electrification.* **2024**, *10*, 4542–4570. [\[CrossRef\]](#)
60. Ramoliya, F.; Gupta, R.; Darji, K.; Trivedi, C.; Kakkar, R.; Tanwar, S.; Guizani, M. A green IoT-integrated AI-based EV scheduling scheme for efficient charging station selection. In Proceedings of the 2024 International Wireless Communications and Mobile Computing (IWCMC), Ayia Napa, Cyprus, 27–31 May 2024; pp. 327–332.
61. Okuyama, T.; Gonsalves, T.; Upadhyay, J. Autonomous driving system based on deep Q learning. In Proceedings of the 2018 International Conference on Intelligent Autonomous Systems (ICoIAS), Singapore, 1–3 March 2018; pp. 201–205.
62. Mohamed, A.A.S.; Shaier, A.A.; Metwally, H.; Selem, S.I. Wireless charging technologies for electric vehicles: Inductive, capacitive, and magnetic gear. *IET Power Electron.* **2023**, *17*, 3139–3165. [\[CrossRef\]](#)
63. Wu, H.H.; Gilchrist, A.; Sealy, K.D.; Bronson, D. A high efficiency 5 kW inductive charger for EVs using dual side control. *IEEE Trans. Ind. Informat.* **2012**, *8*, 585–595. [\[CrossRef\]](#)
64. Sinha, S.; Kumar, A.; Regensburger, B.; Afridi, K.K. A new design approach to mitigating the effect of parasitics in capacitive wireless power transfer systems for electric vehicle charging. *IEEE Trans. Transport. Electrification.* **2019**, *5*, 1040–1059. [\[CrossRef\]](#)
65. Wang, Y.; Zhang, H.; Cao, Y.; Lu, F. Remaining opportunities in capacitive power transfer based on duality with inductive power transfer. *IEEE Trans. Transp. Electrification.* **2023**, *9*, 2902–2915. [\[CrossRef\]](#)
66. Sallan, J.; Villa, J.L.; Llombart, A.; Sanz, J.F. Optimal design of ICPT systems applied to electric vehicle battery charge. *IEEE Trans. Ind. Electron.* **2009**, *56*, 2140–2149. [\[CrossRef\]](#)
67. Gu, L.; Zulauf, G.; Stein, A.; Kyaw, P.A.; Chen, T.; Davila, J.M. 6.78-MHz wireless power transfer with self-resonant coils at 95% DC–DC efficiency. *IEEE Trans. Power Electron.* **2021**, *36*, 2456–2460. [\[CrossRef\]](#)
68. Zhang, Y.; Yan, Z.; Kan, T.; Zeng, X.; Chen, S.; Mi, C.C. Modeling and analysis of a strongly coupled series–parallel-compensated wireless power transfer system. *IEEE J. Emerg. Sel. Topics Power Electron.* **2019**, *7*, 1364–1370. [\[CrossRef\]](#)
69. Kuperman, A. Additional two-capacitor basic compensation topologies for resonant inductive WPT links. *IEEE Trans. Power Deliv.* **2020**, *35*, 2568–2570. [\[CrossRef\]](#)
70. Komaru, T.; Akita, H. Positional characteristics of capacitive power transfer as a resonance coupling system. In Proceedings of the 2013 IEEE Wireless Power Transfer (WPT), Perugia, Italy, 15–16 May 2013; pp. 218–221.
71. IEC 61980; Electric Vehicle Wireless Power Transfer (WPT) Systems. IEC: London, UK, 2020.
72. SAE J2954_202408; Wireless Power Transfer for Light-Duty Plug-in/Electric Vehicles and Alignment Methodology. SAE International: Warrendale, PA, USA, 2024.
73. SAE J2954/2_202212; Wireless Power Transfer for Heavy-Duty Electric Vehicles. SAE International: Warrendale, PA, USA, 2022.
74. Longo, M.; Zaninelli, D.; Cipriani, G.; Di Dio, V.; Miceli, R. Economic assessments on the use of wired and wireless recharging systems in Italian and European market. In Proceedings of the 2017 AEIT International Annual Conference, Cagliari, Italy, 20–22 September 2017; pp. 1–5.
75. Takanashi, H.; Sato, Y.; Kaneko, Y.; Abe, S.; Yasuda, T. A large air gap 3 kW wireless power transfer system for electric vehicles. In Proceedings of the 2012 IEEE Energy Conversion Congress and Exposition (ECCE), Raleigh, NC, USA, 15–20 September 2012; pp. 269–274.

76. Yang, Y.; El Baghdadi, M.; Lan, U.; Benomar, Y.; Van Mierlo, J.; Hegazy, O. Design methodology modeling and comparative study of wireless power transfer systems for electric vehicles. *Energies* **2018**, *11*, 1716. [CrossRef]
77. Li, W.; Zhao, H.; Li, S.; Deng, J.; Kan, T.; Mi, C.C. Integrated LCC compensation topology for wireless charger in electric and plug-in electric vehicles. *IEEE Trans. Ind. Electron.* **2015**, *62*, 4215–4225. [CrossRef]
78. Chowdhury, S.; Tarek, M.T.B.; Sozer, Y. Design of a 7.7 kW three-phase wireless charging system for light duty vehicles based on overlapping windings. In Proceedings of the 2020 IEEE Energy Conversion Congress and Exposition (ECCE), Detroit, MI, USA, 11–15 October 2020; pp. 5169–5176.
79. Mohammad, M.; Pries, J.; Onar, O.; Galigekere, V.P.; Su, G.-J.; Anwar, S.; Wilkins, J.; Kavimandan, U.D.; Patil, D. Design of an EMF suppressing magnetic shield for a 100-kW dd-coil wireless charging system for electric vehicles. In Proceedings of the 2019 IEEE Applied Power Electronics Conference and Exposition (APEC), Anaheim, CA, USA, 17–21 March 2019; pp. 1521–1527.
80. Tritschler, J.; Reichert, S.; Goeldi, B. A practical investigation of a high power, bidirectional charging system for electric vehicles. In Proceedings of the 2014 16th European Conference on Power Electronics and Applications, Lappeenranta, Finland, 26–28 August 2014; pp. 1–7.
81. Bojarski, M.; Asa, E.; Colak, K.; Czarkowski, D. A 25 kW industrial prototype wireless electric vehicle charger. In Proceedings of the 2016 IEEE Applied Power Electronics Conference and Exposition (APEC), Long Beach, CA, USA, 20–24 March 2016; pp. 1756–1761.
82. Bosshard, R.; Kolar, J.W. Multi-objective optimization of 50 kW/85 kHz IPT system for public transport. *IEEE J. Emerg. Sel. Top. Power Electron.* **2016**, *4*, 1370–1382. [CrossRef]
83. Galigekere, V.P.; Pries, J.; Onar, O.C.; Su, G.J.; Anwar, S.; Wiles, R.; Seiber, L.; Wilkins, J. Design and implementation of an optimized 100 kW stationary wireless charging system for EV battery recharging. In Proceedings of the 2018 IEEE Energy Conversion Congress and Exposition (ECCE), Portland, OR, USA, 23–27 September 2018; pp. 3587–3592.
84. KAIST OLEV Team. *Feasibility Studies of On-Line Electric Vehicle (OLEV) Project*; Internal Report; KAIST: Daejeon, Republic of Korea, 2009.
85. Choi, S.Y.; Gu, B.W.; Jeong, S.Y.; Rim, C.T. Advances in wireless power transfer systems for roadway-powered electric vehicles. *IEEE J. Emerg. Sel. Topics Power Electron.* **2015**, *3*, 18–36. [CrossRef]
86. INTIS. INTIS-Integrated Infrastructure Solutions. Available online: <https://www.intis.de/wireless-power-transfer.html> (accessed on 18 December 2024).
87. INTIS. Available online: https://www.intis.de/assets/ecartec2014_e.pdf (accessed on 18 December 2024).
88. DC Streetcar. Available online: <https://dcstreetcar.com/wp-content/uploads/2020/10/Section-D-Part-6-723-830-pagesred.pdf> (accessed on 18 December 2024).
89. Kim, J.H.; Lee, B.-S.; Lee, J.-H.; Lee, S.-H.; Park, C.-B.; Jung, S.-M.; Lee, S.-G.; Yi, K.-P.; Baek, J. Development of 1-MW inductive power transfer system for a high-speed train. *IEEE Trans. Ind. Electron.* **2015**, *62*, 6242–6250. [CrossRef]
90. Villar, I.; Garcia-Bediaga, A.; Iruretagoyena, U.; Arregi, R.; Estevez, P. Design and experimental validation of a 50 kW IPT for Railway Traction Applications. In Proceedings of the 2018 IEEE Energy Conversion Congress and Exposition (ECCE), Portland, OR, USA, 23–27 September 2018; pp. 1177–1183.
91. Mi, C.C.; Buja, G.; Choi, S.Y.; Rim, C.T. Modern advances in wireless power transfer systems for roadway powered electric vehicles. *IEEE Trans. Ind. Electron.* **2016**, *63*, 6533–6545. [CrossRef]
92. Throngnumchai, K.; Hanamura, A.; Naruse, Y.; Takeda, K. Design and evaluation of a wireless power transfer system with road embedded transmitter coils for dynamic charging of electric vehicles. In Proceedings of the 2013 World Electric Vehicle Symposium and Exhibition (EVS27), 17–20 November 2013; pp. 1–10.
93. Buja, G.; Bertoluzzo, M.; Dashora, H.K. Lumped track layout design for dynamic wireless charging of electric vehicles. *IEEE Trans. Ind. Electron.* **2016**, *63*, 6631–6640. [CrossRef]
94. Zhang, X.; Yuan, Z.; Yang, Q.; Li, Y.; Zhu, J.; Li, Y. Coil design and efficiency analysis for dynamic wireless charging system for electric vehicles. *IEEE Trans. Magn.* **2016**, *52*, 8700404. [CrossRef]
95. Bertoluzzo, M.; Buja, G.; Dashora, H.K. Design of DWC system track with unequal DD coil set. *IEEE Trans. Transp. Electrific.* **2017**, *3*, 380–391. [CrossRef]
96. Tavakoli, R.; Dede, E.M.; Chou, C.; Pantic, Z. Cost-efficiency optimization of ground assemblies for dynamic wireless charging of electric vehicles. *IEEE Trans. Transp. Electrific.* **2022**, *8*, 734–751. [CrossRef]
97. Chen, W.; Lin, F.; Covic, G.A. A modified DDQ track for interoperable EV dynamic charging. *IEEE Trans. Power Electron.* **2023**, *38*, 11738–11750. [CrossRef]
98. Bagchi, A.C.; Kamineni, A.; Zane, R.A.; Carlson, R. Review and comparative analysis of topologies and control methods in dynamic wireless charging of electric vehicles. *IEEE J. Emerg. Sel. Top. Power Electron.* **2021**, *9*, 4947–4962. [CrossRef]
99. Tavakoli, R.; Pantic, Z. Analysis, design, and demonstration of a 25-kW dynamic wireless charging system for roadway electric vehicles. *IEEE J. Emerg. Sel. Top. Power Electron.* **2018**, *6*, 1378–1393. [CrossRef]

100. Zhou, Z.; Zhang, L.; Liu, Z.; Chen, Q.; Long, R.; Su, H. Model predictive control for the receiving-side DC–DC converter of dynamic wireless power transfer. *IEEE Trans. Power Electron.* **2020**, *35*, 8985–8997. [[CrossRef](#)]
101. Liu, J.; Liu, Z.; Su, H. Passivity-based PI control for receiver side of dynamic wireless charging system in electric vehicles. *IEEE Trans. Ind. Electron.* **2022**, *69*, 783–794. [[CrossRef](#)]
102. Zhang, M.; Liu, Z.; Su, H. Precise disturbance rejection for dynamic wireless charging system of electric vehicle using internal model-based regulator with disturbance observer. *IEEE Trans. Ind. Electron.* **2024**, *71*, 7695–7705. [[CrossRef](#)]
103. Li, S.; Mi, C.C. Wireless power transfer for electric vehicle applications. *IEEE J. Emerg. Sel. Top. Power Electron.* **2015**, *3*, 4–17.
104. Rahulkumar, J.; Narayanamoorthi, R. Power control and efficiency enhancement topology for dual receiver wireless power transfer EV quasi-dynamic charging. In Proceedings of the 2023 IEEE International Transportation Electrification Conference (ITEC-India), Chennai, India, 12–15 December 2023; pp. 1–6.
105. Mohamed, A.A.S.; Lashway, C.R.; Mohammed, O. Modeling and feasibility analysis of quasi-dynamic WPT system for EV applications. *IEEE Trans. Transport. Electrific.* **2017**, *3*, 343–353. [[CrossRef](#)]
106. Zhang, B.; Carlson, R.B.; Galigekere, V.P.; Onar, O.C.; Mohammad, M.; Dickerson, C.C.; Walker, L.K. Quasi-dynamic electromagnetic field safety analysis and mitigation for high-power dynamic wireless charging of electric vehicles. In Proceedings of the 2021 IEEE Transportation Electrification Conference & Expo (ITEC), Chicago, IL, USA, 21–25 June 2021; pp. 1–7.
107. Tan, L.; Xie, H.; Wu, Z.; Wang, R.; Huang, X. An optimized power-efficiency coordinated control method for EVs charging and discharging applications. *IEEE Trans. Ind. Electron.* **2023**, *70*, 7257–7267. [[CrossRef](#)]
108. Carmeli, M.S.; Castelli-Dezza, F.; Mauri, M.; Rossi, M.; Dolata, A.; Pedretti, M.; Simonini, I. Analysis of a quasi-dynamic wireless power transfer system for EV batteries charging. In Proceedings of the 2018 International Symposium on Power Electronics, Electrical Drives, Automation and Motion (SPEEDAM), Amalfi, Italy, 20–22 June 2018; pp. 383–388.
109. Karneddi, H.; Ronanki, D. Driving range extension of electric city buses using opportunity wireless charging. In Proceedings of the IECON 2021—47th Annual Conference of the IEEE Industrial Electronics Society, Toronto, ON, Canada, 13–16 October 2021; pp. 1–5.
110. Shafiqurrahman, A.; Khadkikar, V.; Rathore, A.K. Electric vehicle-to-vehicle (V2V) power transfer: Electrical and communication developments. *IEEE Trans. Transport. Electrific.* **2024**, *10*, 6258–6284. [[CrossRef](#)]
111. Liu, W.; Chau, K.T.; Chow, C.C.T.; Lee, C.H.T. Wireless energy trading in traffic internet. *IEEE Trans. Power Electron.* **2022**, *37*, 4831–4841. [[CrossRef](#)]
112. Newbolt, T.; Mandal, P.; Wang, H.; Zane, R. Sustainability of dynamic wireless power transfer roadway for in-motion electric vehicle charging. *IEEE Trans. Transport. Electrific.* **2024**, *10*, 1347–1362. [[CrossRef](#)]
113. Covic, G.A.; Boys, J.T. Modern trends in inductive power transfer for transportation applications. *IEEE J. Emerg. Sel. Top. Power Electron.* **2013**, *1*, 28–41. [[CrossRef](#)]
114. Covic, G.A.; Boys, J.T.; Kissin, M.L.G.; Lu, H.G. A three-phase inductive power transfer system for roadway-powered vehicles. *IEEE Trans. Ind. Electron.* **2007**, *54*, 3370–3378. [[CrossRef](#)]
115. Nagatsuka, Y.; Ehara, N.; Kaneko, Y.; Abe, S.; Yasuda, T. Compact contactless power transfer system for electric vehicles. In Proceedings of the 2010 International Power Electronics Conference-ECCE ASIA-, Sapporo, Japan, 21–24 June 2010; pp. 807–813.
116. Elliott, G.; Raabe, S.; Covic, G.A.; Boys, J.T. Multiphase pickups for large lateral tolerance contactless power-transfer systems. *IEEE Trans. Ind. Electron.* **2010**, *57*, 1590–1598. [[CrossRef](#)]
117. Budhia, M.; Covic, G.A.; Boys, J.T. Design and optimization of circular magnetic structures for lumped inductive power transfer systems. *IEEE Trans. Power Electron.* **2011**, *26*, 3096–3108. [[CrossRef](#)]
118. Budhia, M.; Boys, J.T.; Covic, G.A.; Huang, C.-Y. Development of a single-sided flux magnetic coupler for electric vehicle IPT charging systems. *IEEE Trans. Ind. Electron.* **2013**, *60*, 318–328. [[CrossRef](#)]
119. Bosshard, R.; Iruetagoiena, U.; Kolar, J.W. Comprehensive evaluation of rectangular and double-D coil geometry for 50 kW/85 kHz IPT system. *IEEE J. Emerg. Sel. Top. Power Electron.* **2016**, *4*, 1406–1415. [[CrossRef](#)]
120. Bandyopadhyay, S.; Venugopal, P.; Dong, J.; Bauer, P. Comparison of magnetic couplers for IPT-based EV charging using multi-objective optimization. *IEEE Trans. Veh. Technol.* **2019**, *68*, 5416–5429. [[CrossRef](#)]
121. Covic, G.A.; Kissin, M.L.G.; Kacprzak, D.; Clausen, N.; Hao, H. A bipolar primary pad topology for EV stationary charging and highway power by inductive coupling. In Proceedings of the 2011 IEEE Energy Conversion Congress and Exposition, Phoenix, AZ, USA, 17–22 September 2011; pp. 1832–1838.
122. Kim, S.; Zaheer, A.; Covic, G.; Boys, J. Tripolar pad for inductive power transfer systems. In Proceedings of the IECON 2014—40th Annual Conference of the IEEE Industrial Electronics Society, Dallas, TX, USA, 29 October–1 November 2014; pp. 3066–3072.
123. Tan, P.; Peng, T.; Gao, X.; Zhang, B. Flexible combination and switching control for robust wireless power transfer system with hexagonal array coil. *IEEE Trans. Power Electron.* **2021**, *36*, 3868–3882. [[CrossRef](#)]
124. Kurschner, D.; Rathge, C.; Jumar, U. Design methodology for high efficient inductive power transfer systems with high coil positioning flexibility. *IEEE Trans. Ind. Electron.* **2013**, *60*, 372–381. [[CrossRef](#)]

125. Bosshard, R.; Kolar, J.W.; Muhlethaler, J.; Stevanovic, I.; Wunsch, B.; Canales, F. Modeling and η - α -pareto optimization of inductive power transfer coils for electric vehicles. *IEEE J. Emerg. Sel. Top. Power Electron.* **2015**, *3*, 50–64. [[CrossRef](#)]
126. Hariri, A.; Elsayed, A.; Mohammed, O.A. An integrated characterization model and multi-objective optimization for the design of an EV charger's circular wireless power transfer pads. *IEEE Trans. Magn.* **2017**, *53*, 8001004. [[CrossRef](#)]
127. Zhang, C.; Yao, Y.; Wang, Y. Decoupling optimization of the three-coil coupler for IPT system featuring high efficiency and misalignment tolerance. *IEEE Trans. Ind. Electron.* **2023**, *70*, 8918–8927. [[CrossRef](#)]
128. Qin, R.; Li, J.; Sun, J.; Costinett, D. Shielding design for high-frequency wireless power transfer system for EV charging with self-resonant coils. *IEEE Trans. Power Electron.* **2023**, *38*, 7900–7909. [[CrossRef](#)]
129. Wang, H.; Chau, K.T.; Lee, C.H.T.; Tian, X. Design and analysis of wireless resolver for wireless switched reluctance motors. *IEEE Trans. Ind. Electron.* **2023**, *70*, 2221–2230. [[CrossRef](#)]
130. Liu, W.; Lu, J.; Mi, C.C.; Chau, K.T. Integrated sensorless wireless charging using symmetric high-order network for multistorey car parks. *IEEE Trans. Power Electron.* **2024**, *39*, 10568–10581. [[CrossRef](#)]
131. Mai, J.; Wang, Y.; Yao, Y.; Xu, D. Analysis, design, and optimization of the IPT system with LC filter rectifier featuring high efficiency. *IEEE Trans. Ind. Electron.* **2022**, *69*, 12829–12841. [[CrossRef](#)]
132. Liu, C.; Ge, S.; Guo, Y.; Li, H.; Cai, G. Double-LCL resonant compensation network for electric vehicles wireless power transfer: Experimental study and analysis. *IET Power Electron.* **2016**, *9*, 2262–2270. [[CrossRef](#)]
133. Liu, Z.; Su, M.; Zhu, Q.; Zhao, L.; Hu, A.P. A dual frequency tuning method for improved coupling tolerance of wireless power transfer system. *IEEE Trans. Power Electron.* **2021**, *36*, 7360–7365. [[CrossRef](#)]
134. Lu, F.; Hofmann, H.; Deng, J.; Mi, C. Output power and efficiency sensitivity to circuit parameter variations in double-sided LCC compensated wireless power transfer system. In Proceedings of the 2015 IEEE Applied Power Electronics Conference and Exposition (APEC), Charlotte, NC, USA, 15–19 March 2015; pp. 597–601.
135. Byeon, J.; Kang, M.; Kim, M.; Joo, D.-M.; Lee, B.K. Hybrid control of inductive power transfer charger for electric vehicles using LCCL-S resonant network in limited operating frequency range. In Proceedings of the 2016 IEEE Energy Conversion Congress and Exposition (ECCE), Milwaukee, WI, USA, 18–22 September 2016; pp. 1–6.
136. Liu, F.; Zhang, Y.; Chen, K.; Zhao, Z.; Yuan, L. A comparative study of load characteristics of resonance types in wireless transmission systems. In Proceedings of the 2016 Asia-Pacific International Symposium on Electromagnetic Compatibility (APEMC), Shenzhen, China, 17–21 May 2016; pp. 203–206.
137. Wang, Y.; Yao, Y.; Liu, X.; Xu, D. S/CLC compensation topology analysis and circular coil design for wireless power transfer. *IEEE Trans. Transport. Electrification.* **2017**, *3*, 496–507. [[CrossRef](#)]
138. Kan, T.; Nguyen, T.-D.; White, J.C.; Malhan, R.K.; Mi, C.C. A new integration method for an electric vehicle wireless charging system using LCC compensation topology: Analysis and design. *IEEE Trans. Power Electron.* **2017**, *32*, 1638–1650. [[CrossRef](#)]
139. Li, S.; Li, W.; Deng, J.; Nguyen, T.D.; Mi, C.C. A double-sided LCC compensation network and its tuning method for wireless power transfer. *IEEE Trans. Veh. Technol.* **2015**, *64*, 2261–2273. [[CrossRef](#)]
140. Li, W.; Zhao, H.; Deng, J.; Li, S.; Mi, C.C. Comparison study on SS and double-sided LCC compensation topologies for EV/PHEV wireless chargers. *IEEE Trans. Veh. Technol.* **2016**, *65*, 4429–4439. [[CrossRef](#)]
141. Tao, C.; Wang, L.; Zhang, Y.; Li, S.; Da, C. Research on three-phase hybrid compensation WPT system with high misalignment tolerance and its ZVS control strategy. *IEEE Trans. Power Electron.* **2023**, *38*, 14847–14860. [[CrossRef](#)]
142. Esteban, B.; Sid-Ahmed, M.; Kar, N.C. A comparative study of power supply architectures in wireless EV charging systems. *IEEE Trans. Power Electron.* **2015**, *30*, 6408–6422. [[CrossRef](#)]
143. Yao, Y.; Wang, Y.; Liu, X.; Lin, F.; Xu, D. A novel parameter tuning method for a double-sided LCL compensated WPT system with better comprehensive performance. *IEEE Trans. Power Electron.* **2018**, *33*, 8525–8536. [[CrossRef](#)]
144. Cai, J.; Wu, X.; Sun, P.; Deng, Q.; Sun, J.; Zhou, H. Design of constant-voltage and constant-current output modes of double-sided LCC inductive power transfer system for variable coupling conditions. *IEEE Trans. Power Electron.* **2024**, *39*, 1676–1689. [[CrossRef](#)]
145. Cai, C.; Wang, J.; Fang, Z.; Zhang, P.; Hu, M.; Zhang, J.; Li, L.; Lin, Z. Design and optimization of load-independent magnetic resonant wireless charging system for electric vehicles. *IEEE Access* **2018**, *6*, 17264–17274. [[CrossRef](#)]
146. Campi, T.; Cruciani, S.; Maradei, F.; Feliziani, M. Near-field reduction in a wireless power transfer system using LCC compensation. *IEEE Trans. Electromagn. Compat.* **2017**, *59*, 686–694. [[CrossRef](#)]
147. Park, M.; Nguyen, V.T.; Yu, S.-D.; Yim, S.-W.; Park, K.; Min, B.D.; Kim, S.-D.; Cho, J.G. A study of wireless power transfer topologies for 3.3 kW and 6.6 kW electric vehicle charging infrastructure. In Proceedings of the 2016 IEEE Transportation Electrification Conference and Expo, Asia-Pacific (ITEC Asia-Pacific), Busan, Republic of Korea, 1–4 June 2016; pp. 689–692.
148. Onar, O.C.; Miller, J.M.; Campbell, S.L.; Coomer, C.; White, P.; Seiber, L.E. A novel wireless power transfer for in-motion EV/PHEV charging. In Proceedings of the 2013 Twenty-Eighth Annual IEEE Applied Power Electronics Conference and Exposition (APEC), Long Beach, CA, USA, 17–21 March 2013; pp. 3073–3080.
149. Deng, J.; Li, W.; Nguyen, T.D.; Li, S.; Mi, C.C. Compact and efficient bipolar coupler for wireless power chargers: Design and analysis. *IEEE Trans. Power Electron.* **2015**, *30*, 6130–6140. [[CrossRef](#)]

150. Feng, H.; Cai, T.; Duan, S.; Zhao, J.; Zhang, X.; Chen, C. An LCC-compensated resonant converter optimized for robust reaction to large coupling variation in dynamic wireless power transfer. *IEEE Trans. Ind. Electron.* **2016**, *63*, 6591–6601. [[CrossRef](#)]
151. Li, Y.; Sun, W.; Liu, J.; Liu, Y.; Yang, X.; Li, Y.; Hu, J.; He, Z. A new magnetic coupler with high rotational misalignment tolerance for unmanned aerial vehicles wireless charging. *IEEE Trans. Power Electron.* **2022**, *37*, 12986–12991. [[CrossRef](#)]
152. Liu, N.; Habetler, T.G. Design of a universal inductive charger for multiple electric vehicle models. *IEEE Trans. Power Electron.* **2015**, *30*, 6378–6390. [[CrossRef](#)]
153. Vu, V.B.; Ramezani, A.; Triviño, A.; González-González, J.M.; Kadandani, N.B.; Dahidah, M.; Pickert, V.; Narimani, M.; Aguado, J. Operation of inductive charging systems under misalignment conditions: A review for electric vehicles. *IEEE Trans. Transp. Electrification.* **2023**, *9*, 1857–1887. [[CrossRef](#)]
154. Villa, J.L.; Sallan, J.; Osorio, J.F.S.; Llombart, A. High-misalignment tolerant compensation topology for ICPT systems. *IEEE Trans. Ind. Electron.* **2012**, *59*, 945–951. [[CrossRef](#)]
155. Ramezani, A.; Narimani, M. Optimized electric vehicle wireless chargers with reduced output voltage sensitivity to misalignment. *IEEE J. Emerg. Sel. Top. Power Electron.* **2020**, *8*, 3569–3581. [[CrossRef](#)]
156. Zhao, L.; Thrimawithana, D.J.; Madawala, U.K.; Hu, A.P.; Mi, C.C. A misalignment-tolerant series-hybrid wireless EV charging system with integrated magnetics. *IEEE Trans. Power Electron.* **2019**, *34*, 1276–1285. [[CrossRef](#)]
157. Qu, X.; Yao, Y.; Wang, D.; Wong, S.-C.; Tse, C.K. A family of hybrid IPT topologies with near load-independent output and high tolerance to pad misalignment. *IEEE Trans. Power Electron.* **2020**, *35*, 6867–6877. [[CrossRef](#)]
158. Chen, Y.; He, S.; Yang, B.; Chen, S.; He, Z.; Mai, R. Reconfigurable rectifier-based detuned series-series compensated IPT system for anti-misalignment and efficiency improvement. *IEEE Trans. Power Electron.* **2023**, *38*, 2720–2729. [[CrossRef](#)]
159. Zhang, Y.; Pan, W.; Wang, H.; Shen, Z.; Wu, Y.; Dong, J.; Mao, X. Misalignment-tolerant dual-transmitter electric vehicle wireless charging system with reconfigurable topologies. *IEEE Trans. Power Electron.* **2022**, *37*, 8816–8819. [[CrossRef](#)]
160. Mai, J.; Wang, Y.; Yao, Y.; Xu, D. Analysis and design of high-misalignment-tolerant compensation topologies with constant-current or constant-voltage output for IPT systems. *IEEE Trans. Power Electron.* **2021**, *36*, 2685–2695. [[CrossRef](#)]
161. Zhu, Q.; Guo, Y.; Wang, L.; Liao, C.; Li, F. Improving the misalignment tolerance of wireless charging system by optimizing the compensate capacitor. *IEEE Trans. Ind. Electron.* **2015**, *62*, 4832–4836. [[CrossRef](#)]
162. Wei, Z.; Zhang, B.; Lin, S.; Wang, C. A self-oscillation WPT system with high misalignment tolerance. *IEEE Trans. Power Electron.* **2024**, *39*, 1870–1887. [[CrossRef](#)]
163. Miller, J.M.; Onar, O.C.; Chinthavali, M. Primary-side power flow control of wireless power transfer for electric vehicle charging. *IEEE J. Emerg. Sel. Top. Power Electron.* **2015**, *3*, 147–162. [[CrossRef](#)]
164. Zhang, Z.; Zhu, F.; Xu, D.; Krein, P.T.; Ma, H. An integrated inductive power transfer system design with a variable inductor for misalignment tolerance and battery charging applications. *IEEE Trans. Power Electron.* **2020**, *35*, 11544–11556. [[CrossRef](#)]
165. Dai, X.; Li, X.; Li, Y.; Hu, A.P. Maximum efficiency tracking for wireless power transfer systems with dynamic coupling coefficient estimation. *IEEE Trans. Power Electron.* **2018**, *33*, 5005–5015. [[CrossRef](#)]
166. Berger, A.; Agostinelli, M.; Vesti, S.; Oliver, J.A.; Cobos, J.A.; Huemer, M. A wireless charging system applying phase-shift and amplitude control to maximize efficiency and extractable power. *IEEE Trans. Power Electron.* **2015**, *30*, 6338–6348. [[CrossRef](#)]
167. Fang, Y.; Pong, B.M.H.; Hui, R.S.Y. An enhanced multiple harmonics analysis method for wireless power transfer systems. *IEEE Trans. Power Electron.* **2020**, *35*, 1205–1216. [[CrossRef](#)]
168. Chen, F.; Garnier, H.; Deng, Q.; Kazimierczuk, M.K.; Zhuan, X. Control-oriented modeling of wireless power transfer systems with phase shift control. *IEEE Trans. Power Electron.* **2020**, *35*, 2119–2134. [[CrossRef](#)]
169. Jiang, Y.; Wang, L.; Wang, Y.; Liu, J.; Li, X.; Ning, G. Analysis, design, and implementation of accurate ZVS angle control for EV battery charging in wireless high-power transfer. *IEEE Trans. Ind. Electron.* **2019**, *66*, 4075–4085. [[CrossRef](#)]
170. Liu, W.; Chau, K.T.; Lee, C.H.T.; Jiang, C.; Han, W.; Lam, W.H. A wireless dimmable lighting system using variable-power variable-frequency control. *IEEE Trans. Ind. Electron.* **2020**, *67*, 8392–8404. [[CrossRef](#)]
171. Hua, Z.; Chau, K.T.; Liu, W.; Tian, X. Pulse frequency modulation for parity-time-symmetric wireless power transfer system. *IEEE Trans. Magn.* **2022**, *58*, 1–5. [[CrossRef](#)]
172. Zhou, J.; Guidi, G.; Ljøkelset, K.; Suul, J.A. Evaluation and suppression of oscillations in inductive power transfer systems with constant voltage load and pulse skipping modulation. *IEEE Trans. Power Electron.* **2023**, *38*, 10412–10425. [[CrossRef](#)]
173. Wu, D.; Mai, R.; Zhou, W.; Liu, Y.; Peng, F.; Zhao, S.; Zhou, Q. An improved pulse density modulator in inductive power transfer system. *IEEE Trans. Power Electron.* **2022**, *37*, 12805–12813. [[CrossRef](#)]
174. Hua, Z.; Chau, K.T.; Han, W.; Liu, W.; Ching, T.W. Output-controllable efficiency-optimized wireless power transfer using hybrid modulation. *IEEE Trans. Ind. Electron.* **2022**, *69*, 4627–4636. [[CrossRef](#)]
175. Liu, W.; Chau, K.T.; Lee, C.H.T.; Han, W.; Tian, X.; Lam, W.H. Full range soft-switching pulse frequency modulated wireless power transfer. *IEEE Trans. Power Electron.* **2020**, *35*, 6533–6547. [[CrossRef](#)]
176. Liu, W.; Chau, K.T.; Lee, C.H.T.; Tian, X.; Jiang, C. Hybrid frequency pacing for high-order transformed wireless power transfer. *IEEE Trans. Power Electron.* **2021**, *36*, 1157–1170. [[CrossRef](#)]

177. Wang, X.; Leng, M.; Zhang, X.; Ma, H.; Guo, B.; Xu, J.; Lee, C.K. Synthesis and analysis of primary high-order compensation topologies for wireless charging system applying sub-harmonic control. *IEEE Trans. Power Electron.* **2023**, *38*, 9173–9182. [[CrossRef](#)]
178. Tang, J.; Zhang, Q.; Cui, C.; Na, T.; Hu, T. An improved hybrid frequency pacing modulation for wireless power transfer systems. *IEEE Trans. Power Electron.* **2021**, *36*, 12365–12374. [[CrossRef](#)]
179. Guo, J.; Chau, K.T.; Liu, W.; Hua, Z.; Li, S. Segmented-vector pulse frequency modulated three-level converter for wireless power transfer. *IEEE Trans. Power Electron.* **2024**, *39*, 8959–8972. [[CrossRef](#)]
180. Mishima, T.; Lai, C.-M. Load-adaptive resonant frequency-tuned D-R pulse density modulation for class-D ZVS high-frequency inverter based inductive wireless power transfer. *IEEE Trans. Emerg. Sel. Topics Ind. Electron.* **2022**, *3*, 411–420. [[CrossRef](#)]
181. Sheng, X.; Shi, L. An improved pulse density modulation strategy based on harmonics for ICPT system. *IEEE Trans. Power Electron.* **2020**, *35*, 6810–6819. [[CrossRef](#)]
182. Esteve, V.; Jordan, J.; Sanchis-Kilders, E.; Dede, E.J.; Maset, E.; Ejea, J.B.; Ferreres, A. Enhanced pulse-density-modulated power control for high frequency induction heating inverters. *IEEE Trans. Ind. Electron.* **2015**, *62*, 6905–6914. [[CrossRef](#)]
183. Li, H.; Fang, J.; Chen, S.; Wang, K.; Tang, Y. Pulse density modulation for maximum efficiency point tracking of wireless power transfer systems. *IEEE Trans. Power Electron.* **2018**, *33*, 5492–5501. [[CrossRef](#)]
184. Li, H.; Wang, K.; Fang, J.; Tang, Y. Pulse density modulated ZVS full-bridge converters for wireless power transfer systems. *IEEE Trans. Power Electron.* **2019**, *34*, 369–377. [[CrossRef](#)]
185. Li, H.; Chen, S.; Fang, J.; Tang, Y.; de Rooij, M.A. A low-subharmonic, full-range, and rapid pulse density modulation strategy for ZVS full-bridge converters. *IEEE Trans. Power Electron.* **2019**, *34*, 8871–8881. [[CrossRef](#)]
186. Fan, M.; Shi, L.; Yin, Z.; Jiang, L.; Zhang, F. Improved pulse density modulation for semi-bridgeless active rectifier in inductive power transfer system. *IEEE Trans. Power Electron.* **2019**, *34*, 5893–5902. [[CrossRef](#)]
187. Yenil, V.; Cetin, S. An improved pulse density modulation control for secondary side controlled wireless power transfer system using LCC-S compensation. *IEEE Trans. Ind. Electron.* **2022**, *69*, 12762–12772. [[CrossRef](#)]
188. Zhou, J.; Guidi, G.; Chen, S.; Tang, Y.; Suul, J.A. Conditional pulse density modulation for inductive power transfer systems. *IEEE Trans. Power Electron.* **2024**, *39*, 88–93. [[CrossRef](#)]
189. Wang, X.; Jiang, C.Q.; Zhou, J.; Wang, Y.; Mo, L. Hybrid control based on pulse density modulation and asymmetrical voltage cancellation for WPT systems. *IEEE Trans. Ind. Electron.* **2024**, early access. [[CrossRef](#)]
190. Tang, J.; Na, T.; Zhang, Q. A novel full-bridge step density modulation for wireless power transfer systems. *IEEE Trans. Power Electron.* **2023**, *38*, 41–45. [[CrossRef](#)]
191. Guo, J.; Chau, K.T.; Liu, W.; Hou, Y.; Chan, W.L. Pulse magnitude modulation and token rotation-based voltage balancing method of multilevel inverter for wireless power transfer. *IEEE Trans. Power Electron.* **2024**, early access. [[CrossRef](#)]
192. Jiwariyavej, V.; Imura, T.; Hori, Y. Coupling coefficients estimation of wireless power transfer system via magnetic resonance coupling using information from either side of the system. *IEEE J. Emerg. Sel. Top. Power Electron.* **2015**, *3*, 191–200. [[CrossRef](#)]
193. Chow, J.P.-W.; Chung, H.S.-H.; Cheng, C.-S. Use of transmitter-side electrical information to estimate mutual inductance and regulate receiver-side power in wireless inductive link. *IEEE Trans. Power Electron.* **2016**, *31*, 6079–6091. [[CrossRef](#)]
194. Yang, Y.; Tan, S.C.; Hui, S.Y.R. Fast hardware approach to determining mutual coupling of series-series-compensated wireless power transfer systems with active rectifiers. *IEEE Trans. Power Electron.* **2020**, *35*, 11026–11038. [[CrossRef](#)]
195. Wang, L.; Sun, P.; Wu, X.; Cai, J.; Deng, Q.; Sun, J.; Zhou, H. Mutual inductance identification of IPT system based on soft-start process. *IEEE Trans. Power Electron.* **2022**, *37*, 7504–7517. [[CrossRef](#)]
196. Mohammad, M.; Choi, S. Sensorless estimation of coupling coefficient based on current and voltage harmonics analysis for wireless charging system. In Proceedings of the 2017 IEEE Energy Conversion Congress and Exposition (ECCE), Cincinnati, OH, USA, 1–5 October 2017; pp. 2767–2772.
197. Hu, J.; Zhao, J.; Cui, C. A wide charging range wireless power transfer control system with harmonic current to estimate the coupling coefficient. *IEEE Trans. Power Electron.* **2021**, *36*, 5082–5094. [[CrossRef](#)]
198. Dai, X.; Jiang, J.; Xu, Z.; Li, Y. Cooperative control for multi-excitation units WPT system with multiple coupling parameter identification and area adaptation. *IEEE Access* **2020**, *8*, 38728–38741. [[CrossRef](#)]
199. Su, Y.; Zhang, H.; Wang, Z.; Hu, A.P.; Chen, L.; Sun, Y. Steady-state load identification method of inductive power transfer system based on switching capacitors. *IEEE Trans. Power Electron.* **2015**, *30*, 6349–6355. [[CrossRef](#)]
200. Sheng, X.; Shi, L. Mutual inductance and load identification method for inductively coupled power transfer system based on auxiliary inverter. *IEEE Trans. Veh. Technol.* **2020**, *69*, 1533–1541. [[CrossRef](#)]
201. Su, Y.; Chen, L.; Wu, X.; Hu, A.P.; Tang, C.; Dai, X. Load and mutual inductance identification from the primary side of inductive power transfer system with parallel-tuned secondary power pickup. *IEEE Trans. Power Electron.* **2018**, *33*, 9952–9962. [[CrossRef](#)]
202. Dai, R.; Zhou, W.; Chen, Y.; Zhu, Z.; Mai, R. Pulse density modulation based mutual inductance and load resistance identification method for wireless power transfer system. *IEEE Trans. Power Electron.* **2022**, *37*, 9933–9943. [[CrossRef](#)]

203. Guo, Y.; Zhang, Y.; Li, S.; Tao, C.; Wang, L. Load parameter joint identification of wireless power transfer system based on the DC input current and phase-shift angle. *IEEE Trans. Power Electron.* **2020**, *35*, 10542–10553. [[CrossRef](#)]
204. Guo, Y.; Zhang, Y.; Zhang, W.; Wang, L. Battery parameter identification based on wireless power transfer system with rectifier load. *IEEE Trans. Ind. Electron.* **2021**, *68*, 6893–6904. [[CrossRef](#)]
205. Wang, L.; Sun, P.; Liang, Y.; Sun, J.; Wu, X.; Shen, H.; Deng, Q. Joint real-time identification for mutual inductance and load charging parameters of IPT system. *IEEE J. Emerg. Sel. Top. Power Electron.* **2023**, *11*, 4574–4590. [[CrossRef](#)]
206. Li, W.; Wei, G.; Cui, C.; Zhang, X.; Zhang, Q. A double-side self-tuning LCC/S system using a variable switched capacitor based on parameter recognition. *IEEE Trans. Ind. Electron.* **2021**, *68*, 3069–3078. [[CrossRef](#)]
207. Xue, Z.; Niu, S.; Li, X. A simplified multi-vector-based model predictive current control for PMSM with enhanced performance. *IEEE Trans. Transport. Electrification.* **2023**, *9*, 4032–4044. [[CrossRef](#)]
208. Yin, Z.; Dai, X.; Yang, Z.; Shen, Y.; Li, F.; Xiao, D.; Zhao, H. Torque-induced-overshoot reduction inspired compensator for PMSMs using motor-physics embedded gaussian process regression. *IEEE ASME Trans. Mechatron.* **2024**, early access. [[CrossRef](#)]
209. Yin, Z.; Chen, X.; Shen, Y.; Su, X.; Xiao, D.; Abel, D.; Zhao, H. Plant-physics-guided neural network control for permanent magnet synchronous motors. *IEEE J. Sel. Top. Signal Process.* **2024**, early access. [[CrossRef](#)]
210. Xue, Z.; Niu, S.; Chau, A.M.H.; Luo, Y.; Lin, H.; Li, X. Recent advances in multi-phase electric drives model predictive control in renewable energy application: A state-of-the-art review. *World Electric Veh. J.* **2023**, *14*, 44. [[CrossRef](#)]
211. Yin, Z.; Wang, X.; Su, X.; Shen, Y.; Xiao, D.; Zhao, H. A switched ultra-local model-free predictive controller for PMSMs. *IEEE Trans. Power Electron.* **2024**, *39*, 10665–10669. [[CrossRef](#)]
212. Li, X.; Sang, M.; Wei, Z.; Zhang, Z.; Zhu, X.; Wang, Y.; Hua, W. Magnetic shielding design and performance improvement of HTS coil for single HTS-excitation claw-pole field-modulation machine. *IEEE Trans. Appl. Supercond.* **2024**, *34*, 5200609. [[CrossRef](#)]
213. Lyu, R.; Liu, W.; Li, Q.; Chau, K.T. Overview of superconducting wireless power transfer. *Energy Rep.* **2024**, *12*, 4055–4075. [[CrossRef](#)]
214. Ma, J.; Li, Z.; Liu, Y.; Ban, M.; Song, W. Thermal analysis and optimization of the magnetic coupler for wireless charging system. *IEEE Trans. Power Electron.* **2023**, *38*, 16269–16280. [[CrossRef](#)]
215. Liang, C.; Yang, G.; Yuan, F.; Huang, X.; Sun, Y.; Li, J.; Song, K. Modeling and analysis of thermal characteristics of magnetic coupler for wireless electric vehicle charging system. *IEEE Access* **2020**, *8*, 173177–173185. [[CrossRef](#)]
216. Zhang, X.; Hao, C.; Dou, R.; Zhang, P.; Yuan, Z.; Yang, Q. Ferrite pads gap thermal-magnetic evaluation and mitigation for 11.1 kW wireless power transfer. *IEEE Trans. Magn.* **2023**, *59*, 8600806. [[CrossRef](#)]
217. Deng, P.; Tang, C.; Sun, M.; Liu, Z.; Hu, H.; Lin, T. EMI suppression method for LCC-S MC-WPT systems by parameter optimization. *IEEE Trans. Power Electron.* **2024**, *39*, 11134–11147. [[CrossRef](#)]
218. Sim, B.; Jeong, S.; Kim, Y.; Park, S.; Lee, S.; Hong, S.; Song, J.; Kim, H.; Kang, H.; Park, H.; et al. A near field analytical model for EMI reduction and efficiency enhancement using an nth harmonic frequency shielding coil in a loosely coupled automotive WPT system. *IEEE Trans. Electromagn. Compat.* **2021**, *63*, 935–946. [[CrossRef](#)]
219. Wang, Q.; Li, W.; Kang, J.; Wang, Y. Electromagnetic safety evaluation and protection methods for a wireless charging system in an electric vehicle. *IEEE Trans. Electromagn. Compat.* **2019**, *61*, 1913–1925. [[CrossRef](#)]
220. Park, S. Evaluation of Electromagnetic Exposure During 85 kHz Wireless Power Transfer for Electric Vehicles. *IEEE Trans. Magn.* **2018**, *54*, 5100208. [[CrossRef](#)]

Disclaimer/Publisher’s Note: The statements, opinions and data contained in all publications are solely those of the individual author(s) and contributor(s) and not of MDPI and/or the editor(s). MDPI and/or the editor(s) disclaim responsibility for any injury to people or property resulting from any ideas, methods, instructions or products referred to in the content.